CANADIAN JOURNAL OF RESEARCH

VOLUME 25 MAY, 1947 NUMBER 3

— SECTION A —

PHYSICAL SCIENCES

Contents

NATIONAL RESEARCH COUNCIL
OTTAWA, CANADA

CANADIAN JOURNAL OF RESEARCH

The *Canadian Journal of Research* is issued in six sections, as follows:

A. Physical Sciences
B. Chemical Sciences
C. Botanical Sciences
D. Zoological Sciences
E. Medical Sciences
F. Technology

For the present, each of these sections is to be issued six times annually, under separate cover, with separate pagination.

The *Canadian Journal of Research* is published by the National Research Council of Canada under authority of the Chairman of the Committee of the Privy Council on Scientific and Industrial Research. The *Canadian Journal of Research* is edited by a joint Editorial Board consisting of members of the National Research Council of Canada, the Royal Society of Canada, and the Chemical Institute of Canada.

Sections B and F of the *Canadian Journal of Research* have been chosen by the Chemical Institute of Canada as its medium of publication for scientific papers.

Manuscripts should be addressed:

Editor-in-Chief,
Canadian Journal of Research,
National Research Council, Ottawa, Canada.

Canadian Journal of Research

Issued by THE NATIONAL RESEARCH COUNCIL OF CANADA

VOL. 25, SEC. A. MAY, 1947 NUMBER 3

A NOTE ON THE ELECTRON MICROSCOPE EXAMINATION OF GREASES[1]

BY S. G. ELLIS[2]

Abstract

A method is described for examining the soap component of lubricating greases with the electron microscope. The soap component is mounted on Formvar films from a dispersion in ether. The specimen is shadow cast by the method of Williams and Wyckoff. The deduction of the shape of the soap particles is discussed.

Introduction

For the purpose of this note a grease is considered as a suspension of soap particles in oil. The properties of the grease that are of commercial importance, such, for instance, as the viscosity, depend in part on the form, number, and mode of aggregation of the soap particles. These, in turn, depend on the chemical nature of the soap and the thermal and mechanical treatment of the grease during manufacture.

The prime problem to be solved by the electron microscopic examination of the grease is the determination of the size and shape of the soap particles. Since the oil components of the grease, if of sufficiently high vapour pressure, will evaporate in the electron microscope, any conclusions as to the state of aggregation of the soap particles in the grease must be inferred from the micrographs of the residual soap component.

The electron microscopic examination may be considered in three stages, the preparation of the specimen, the production of the micrograph, and the interpretation of the micrograph. This is a subdivision for convenience of discussion, since the deductions made in the last stage must be influenced by what has been done in the previous two stages. For this reason it is desirable, as a matter of practice, for one person to perform all these stages of the work.

Previous Work

In early work by Drs. Beatrice M. Deacon, L. Newman, and J. H. L. Watson at this laboratory the specimens were prepared by the following method. A film of 'Formvar' about 200 Å thick was formed on a glass

[1] *Manuscript received July 3, 1946.*

Contribution from the McLennan Laboratory, Department of Physics, University of Toronto, Toronto, Ont. Section D (a) of a thesis submitted in partial fulfilment of the requirements governing the award of the degree of Doctor of Philosophy at the University of Toronto.

[2] *Holder of a Fellowship under the National Research Council of Canada, 1945-1946.*

microscope slide by the usual method (3). A small amount of grease (less than 10^{-3} cc.) was placed on this film, while it was still attached to the glass slide, and was spread out with either a razor blade or a camel's-hair brush. Alternatively it can be squashed and smeared out with a dust-free microscope cover slide. The Formvar film was then cut, floated off on to water, picked up and transferred to a 200 mesh screen, with the grease side away from the screen. The films were manipulated to bring the edges of the grease smears over the mesh in order to obtain areas thin enough to transmit electrons. Preliminary examination of the mounted specimens under a dark field light microscope at ×100 aided in selecting suitable mounts. The specimens were examined in the first electron microscope built in this laboratory (2), without the aid of an aperture limiting diaphragm in the objective.

Two difficulties were encountered with this method of mounting. It was not easy to mount the specimens by this method without tearing the Formvar film, and the micrographs were difficult to interpret.

Later Work

All the micrographs shown in this note are of the same grease sample. It is chosen, here, because it led to unusual difficulties of interpretation. The soap is a calcium base soap.

Fig. 1 was obtained by the method described above. It is seen that this soap exists in a fibre form with a periodic variation in either thickness or density along the fibre. From our knowledge of soaps the variation in thickness would appear to be more probable. The spacing of the spots is not uniform but is of the order 1100 Å. The details of the structure are not resolved, and this is not due to optical deficiencies in the microscope, since holes in the film were sharply focused. In some micrographs the photographic density between the spots was the same as that of the general background due to the Formvar film itself.

Since some of the lack of contrast in the micrographs might be due to low vapour pressure components of the oil remaining on the film in the microscope, the grease was mounted from a suspension in ether.

Formvar films, 200 Å thick, mounted on meshes, were attached film up, to a glass microscope slide with small spots of rubber cement.* These were chilled by inverting the slide over liquid air and leaving them in the cold air above the liquid for a few minutes. Meanwhile some grease (about 10^{-3} cc.) was taken on a needle and shaken with 2 cc. of ether. The slide with the Formvar films was placed on the bench and breathed upon to coat the Formvar with a thin protective film of moisture. A small drop of the ether suspension

** The dried rubber cement is a good insulator and should not be allowed to enter the electron microscope subsequently.*

FIG. 1. *Electron micrograph of soap fibres from calcium base grease.*

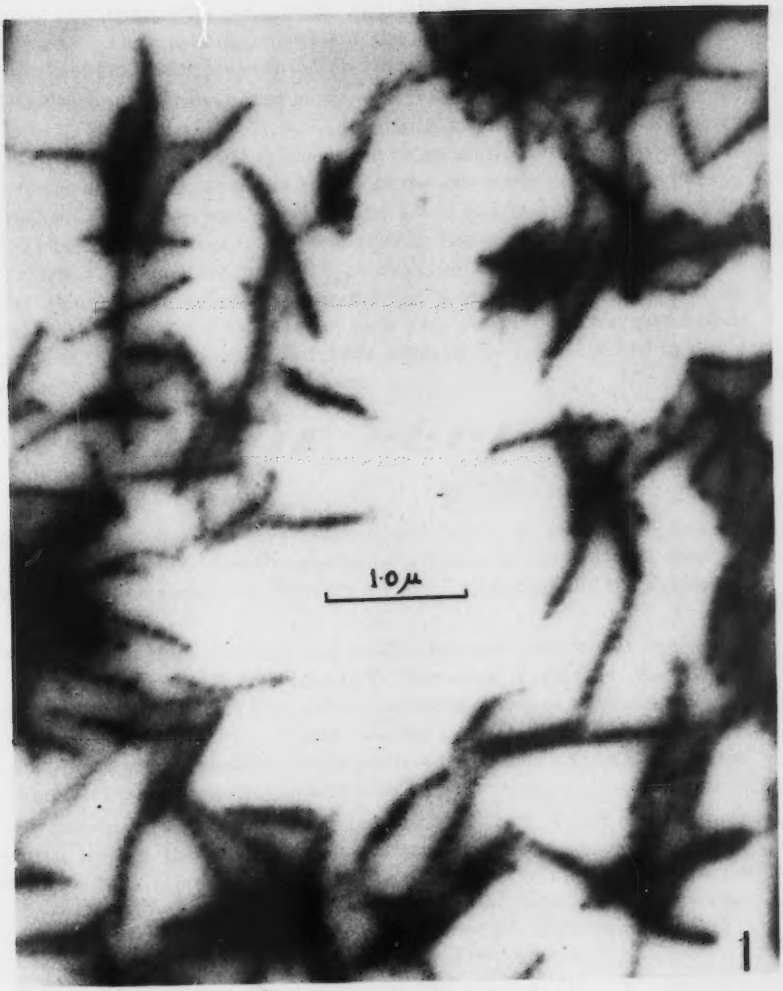
1·0μ
1

(recently shaken) was withdrawn by means of a micropipette and immediately touched to the top of the Formvar film near the edge before the moisture could evaporate, and was immediately blown upon to promote evaporation of the ether. Close to the point at which the ether first touched the film were areas of film destruction but, outside this, suitable deposits of the soap fibres were found. Dark field examination in the light microscope helped in selecting the best mount for the electron microscope.

These mounts were examined in the new 1944 electron microscope designed by Drs. L. Newman and J. H. L. Watson and constructed in this laboratory (1). In this microscope a diaphragm can be accurately centred to the optical axis of the objective near the exit pupil of the lens while the microscope is in operation. These specimens were photographed at a magnification of ×5000 in the electron microscope. The resolution in the micrographs obtained with this method of mounting, and with an objective diaphragm, was very little better than that previously attained with smeared preparations and no objective diaphragm. Two types of fibre were observed. That sketched in Fig. 2 was the more common, but a few fibres of the type sketched in Fig. 3 were found on examining several plates.

FIG. 2.

FIG. 3.

By displacing the objective diaphragm laterally to cut off all but the scattered electrons and thereby producing a dark field image, it was observed that the soap fibres scattered electrons not much more than did the supporting film.

Since the structure was still not readily interpretable it was decided to apply the shadow casting technique of Williams and Wyckoff (4, 5). To this end the soap was mounted from ether suspension on top of a Formvar film on a mesh as described above. It was shadow cast with from 60 Å to 100 Å of chromium to produce shadows from two to four times as long as the height of the fibres. Fig. 4 is a micrograph of such a preparation.

The micrographs of shadow cast preparations (Figs. 4 and 8) have been prepared by the following method. Contact positive transparencies have been made from the original negatives produced in the microscope, and the figures shown here are of prints made from the contact positive transparencies. This is done in order to obtain shadows that are dark in the prints and thus enhance the appearance of relief, and simplify interpretation.

The increase in resolution in the micrograph is evident (Fig. 4). The form of the fibres is that of a two stranded rope. Both right- and left-handed spirals are present in approximately equal proportions. When one of the fibres is straight (see *A* of Fig. 4) it produces the type of image sketched in Fig. 3, in the non-shadow cast preparations.

It is interesting to note that images of the form sketched in Fig. 5 have not been observed with either the smeared or the ether-mounted specimens without shadow casting. Yet the mass distribution of a twisted fibre projected on to a plane perpendicular to the beam of the electron microscope is symmetrical about the projection of the axis of the fibre. This can be seen from Fig. 6, which is an X-ray photograph of a model of a fibre made from Plasticine into which brass filings have been mixed. In this sense the images of Fig. 1 are not of the form to be expected from the two stranded fibres shown in Fig. 4.

To resolve this point a specimen of the grease was mounted by the smearing method and photographed (Fig. 7). The sample was then shadow cast with chromium and the same field photographed again (Fig. 8). It can be seen from Fig. 8 that most of the soap fibres are embedded in the Formvar film.

FIG. 5.

Comparing the two plates it is seen that the embedded parts (*B* of Fig. 7 and *C* of Fig. 8) scatter electrons little more than would the Formvar they have displaced. In many fields of the ether-mounted specimens the fibres are similarly embedded in the film. This may be due to a solvent effect of the ether on the Formvar film. In both cases the embedded parts of the fibres, since they scatter electrons little more than the rest of the Formvar film, contribute little to the image formation. Consequently at points such as *B* in Fig. 7, between the spots, the photographic density in the micrograph does not differ greatly from the general background due to the Formvar film. It was this factor that confused the interpretation of the micrographs from non-shadow cast specimens.

Had the preparations been made on silica films it appears likely that this difficulty would have been avoided.

Location of Fields

The duplication of certain fields of the specimen is best done by mounting the specimen and film on a mesh that has been pierced with three holes as shown in Fig. 9. Nickel or copper meshes are suitable in this application. The holes should be spaced so that they can be seen on the intermediate screen of the microscope. The holes serve both in orienting the mesh in the object cartridge of the microscope, and as reference points for finding any desired part of the specimen. If a sketch map of the image on the intermediate screen is made it aids in finding the same fields again.

FIG. 4. *Electron micrograph of soap fibres from calcium base grease, shadow cast with chromium.*

FIG. 6. *X-ray photograph of model of soap fibre.*

FIG. 7. *Electron micrograph of soap fibres from calcium base grease.*

FIG. 8. *Same field as Fig. 7 after shadow casting with chromium.*

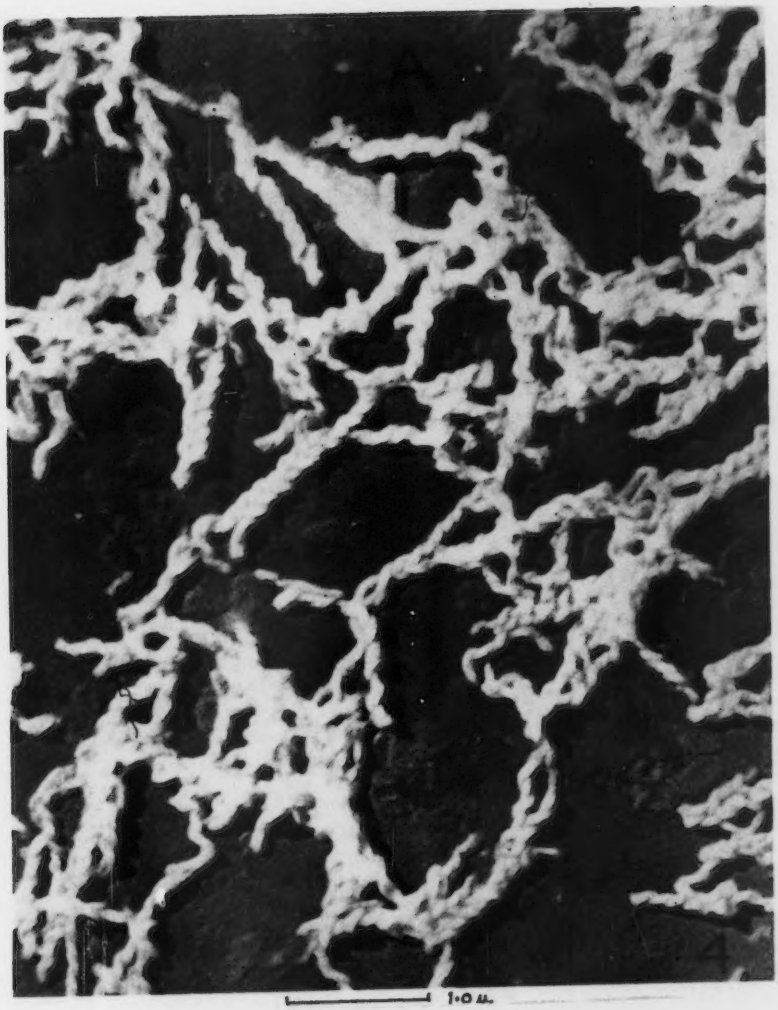
1·0 μ.

PLATE III

6

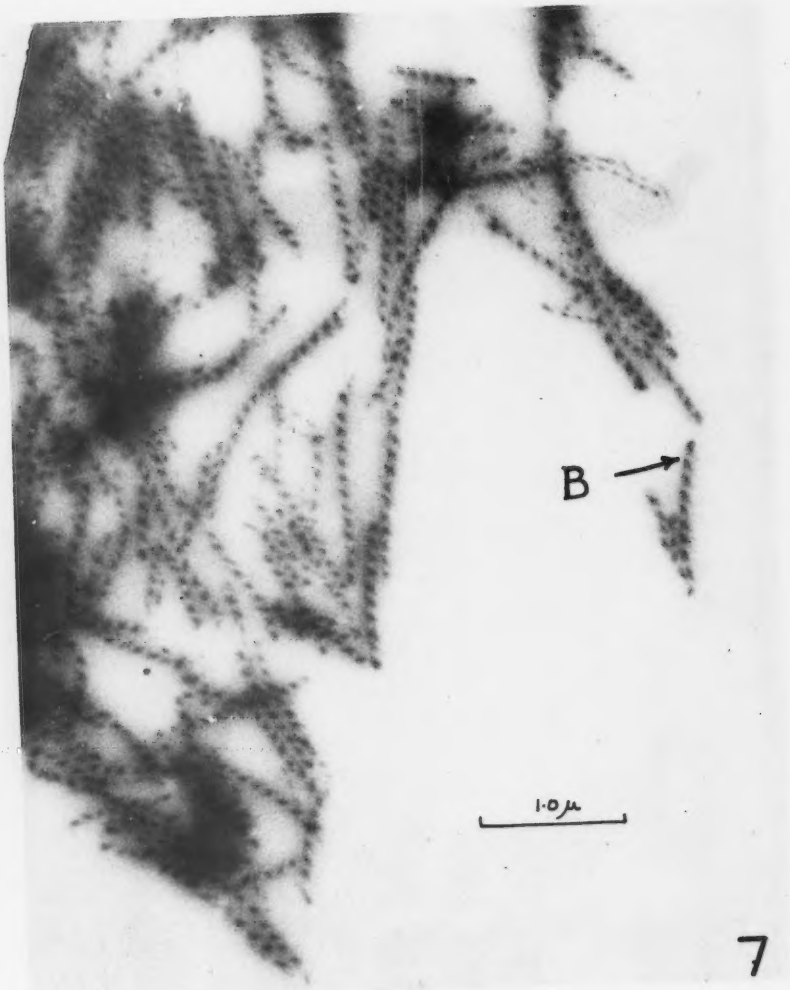
B
1·0μ
7


8

Conclusions

The conclusions as to the nature of these particular soap fibres have been given above as an illustration of the general method. The more general interpretation of the pictures must be made by co-ordinating these results with those of other experiments on the grease, and by extending the studies to other greases. This will be done in a later paper.

The techniques described here are not limited in their applications to greases alone and may aid in the general study of soaps. The study reported here serves to emphasize the importance of care in the interpretation of electron micrographs. This is particularly the case if the specimen scatters

FIG. 9. *Screen pierced to aid in duplication of field.*

electrons only a little more than does the supporting film, or if the film is cast from a suspension of the particles in a solution of Formvar, and some parts of the particles scatter but little more than the Formvar. It is also evident that the value of the shadow casting techniques is by no means limited to study of very small particles.

Acknowledgments

The writer has received much encouragement from Prof. E. F. Burton of this laboratory, and from Mr. L. W. Sproule of Imperial Oil Ltd. of Sarnia, Ont. He is indebted to Dr. R. K. Stratford of Imperial Oil Ltd. for permission to publish these results, and he wishes to thank Dr. Elizabeth Allin who aided in the preparation of Fig. 6. Imperial Oil Ltd. made a grant towards this work.

References

1. BURTON, E. F. and KOHL, W. H. The electron microscope; an introduction to its fundamental principles and applications. 2nd ed. Reinhold Publishing Corporation, New York. 1946.
2. PREBUS, A. and HILLIER, J. Can. J. Research, A, 17 : 49-63. 1939.
3. SCHAEFER, V. J. and HARKER, D. J. Applied Phys. 13 : 427-433. 1942.
4. WILLIAMS, R. C. and WYCKOFF, R. W. G. J. Applied Phys. 15 : 712-716. 1944.
5. WILLIAMS, R. C. and WYCKOFF, R. W. G. J. Applied Phys. 17 : 23-33. 1946.

THE USE OF HIGH PERMEABILITY MATERIALS IN MAGNETOMETERS. THE APPLICATION OF A SATURATED CORE TYPE MAGNETOMETER TO AN AUTOMATIC STEERING CONTROL[1]

By L. D. Armstrong[2]

Abstract

Two types of magnetometers using high permeability materials are described—first, those using a field leaving the material in an unsaturated condition and giving a second harmonic output, and, second, those using the saturated core method, resulting in a peak signal output. The application of the saturated core type magnetometer to the particular problem of an automatic steering control is described in detail.

Introduction

The principle of the use of high permeability materials in apparatus for the detection of small magnetic fields was used extensively during the war years in both U.S.A. and Canada. This paper is based on work done at the National Research Laboratories in Ottawa on magnetometers using transformers with high permeability, low hysteresis core materials as detection elements. The development and application of the unsaturated core type magnetometer was the work chiefly of Dr. A. C. Young* and Mr. C. K. Jones*. The saturated core type was developed and applied to the particular problem of an automatic steering control by the author in conjunction with Dr. D. G. Hurst*.

Magnetometers are devices for measuring some or all of the following:

1. Direction of magnetic fields;
2. Magnitude of magnetic fields;
3. The gradient of a magnetic field;
4. Changes in any of 1, 2, or 3.

The use of the recently developed magnetic materials of very high permeability yields magnetometers more sensitive than those previously available.

The magnetometers herein described consist of two identical open-core transformers, each having primary and secondary windings that are wound over a core of high permeability material. These transformers are mounted parallel to each other, and the secondary windings connected in opposition to each other. If the transformers are excited by an a-c. voltage applied to the primaries, their output will be modified in the presence of an external magnetic field, owing to the magnetic bias imposed on the core material by the external field. This modified output may then be amplified in a suitable amplifier, and recorded or used as desired.

[1] *Manuscript received June 29, 1946.*

Contribution from the Division of Physics and Electrical Engineering, National Research Laboratories, Ottawa, Canada. Issued as N.R.C. No. 1538.

[2] *Physicist.*

* *Physicist, National Research Laboratories, Ottawa, Canada.*

There are two general modes of operation used in this type of magnetometer. The a-c. voltage impressed on the primary may be such as to saturate the core material twice during each cycle, or it may be small enough to leave the core always in an unsaturated condition.

For ferromagnetic material operated upon by an alternating magnetic field and in the absence of a steady magnetic field, the flux B curve may be given by a Fourier series of both sine and cosine odd harmonic terms (1, pp. 173–177).

That is, if B = the flux density associated with a current $i = i_0 \sin \omega t$ then

$$B = A_1 \cos \omega t + A_3 \cos 3\omega t + A_n \cos n\omega t + C_1 \sin \omega t + C_3 \sin 3\omega t + C_n \sin n\omega t, \quad (1)$$

where n is any odd integer.

The addition of a steady magnetic field H_0 results in an unsymmetrical distortion to the original wave form, the equation for which will therefore be modified by the inclusion of even harmonic terms of the form $K H_0 \begin{matrix}\sin \\ \cos\end{matrix} 2M \omega t$, where M is an integer. By maintaining the flux density of the core material well below saturation and suitably choosing the origin, the higher harmonics become of small effect and B can be represented to a first approximation by an even function of the form

$$B_1 = A_1 \cos \omega t + A_3 \cos 3\omega t + K H_0 \cos 2 \omega t. \quad (2)$$

For a transformer with the primary winding in the opposite direction

$$B_2 = - A_1 \cos \omega t - A_3 \cos 3\omega t + K H_0 \cos 2 \omega t. \quad (3)$$

Hence, with two transformers connected with primaries in opposition, and the secondaries in series, and so placed that the same steady magnetic field is imposed on both of them, the net e.m.f. is given by

$$E = E_1 + E_2 = \frac{d}{dt}(B_1 + B_2) = \frac{d}{dt}(2K H_0 \cos 2\omega t) = - 4K H_0 \omega \sin 2\omega t. \quad (4)$$

This is a second harmonic of magnitude directly proportional to H_0, the steady magnetic field through the transformers. As may be noted, the phase of the output depends on the direction of H_0 through the transformers, the phase shift being 180° on reversal of the direction of H_0. Thus, by using a phase sensitive input in an amplifier, the direction of H_0 may be ascertained.

The harmonic distortion of the B curve on the addition of a constant magnetic field is small for ordinary ferromagnetic materials, and consequently the impressed H_0 must be of considerable magnitude for the output E to be significantly affected. However, the permeability of permalloy materials is very great in comparison with that of ordinary iron, and the subsequent effect on B is correspondingly large. Thus, such materials are suitable as cores in equipment for the detection of small magnetic fields or small changes in them.

In practice the output of an unsaturated core magnetometer is a distorted second harmonic chiefly because the equation for B should contain higher harmonics. As saturation is approached the increasing harmonic content adds in such a way as to form a sharp pulse twice for each cycle of the exciting field, and the sign of the pulse is the same each time but dependent on the direction of the constant field. A more satisfactory explanation of the operation of the saturated core type magnetometer is the descriptive one that follows.

In this mode of operation, which was used in the steering control described later in this paper, the transformers operate on a magnetic cycle that carries the core material through saturation and hence brings it to standard states of magnetization twice during each cycle. This method thus eliminates difficulties due to variations in the permanent magnetization of the two cores.

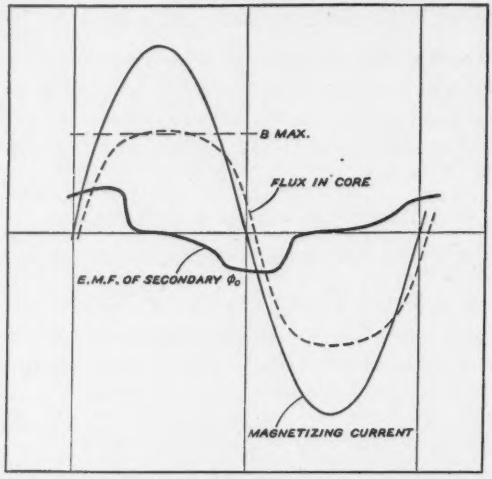

FIG. 1.

Fig. 1 shows a typical magnetization cycle of a core of high permeability material excited approximately to saturation B max. by an exciting field H. Such a magnetization cycle will induce in the secondary winding around the core an e.m.f. having a wave form approximating the curve ϕ_0. The important feature of the induced e.m.f. is the discontinuity, corresponding to the point B max. (Fig. 1) on the magnetization curve, at which point the induced voltage drops from its maximum value rapidly toward zero.

If now a steady external magnetic field is applied along the direction of the axis of the core, the result corresponds to a magnetic bias such that the magnetizing current required to reach saturation is reduced on one half of the cycle and increased on the other half. While the wave form is not fundamentally changed, a shift in the wave pattern results (Fig. 2), the magnitude

of which depends upon the strength of the applied external field and the steepness of the magnetization curve. The time lag of the induced e.m.f. is slightly advanced in one half of the cycle and correspondingly retarded in the other half cycle, the direction and magnitude of the shift depending upon the direction and magnitude of the external field with respect to the impressed magnetizing force.

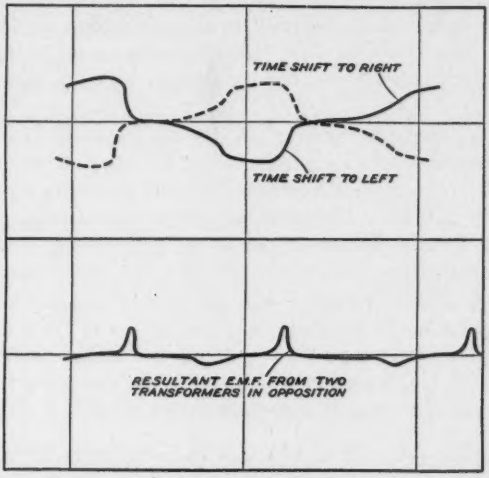

FIG. 2.

If two of these transformers are operated simultaneously and connected so that the induced e.m.f.'s are in opposition, the resulting e.m.f. will be zero when the external field is zero. The application of an external field will, however, result in a phase shift between these induced e.m.f.'s, and the net output will no longer be zero (Fig. 2). The magnitude and direction of the resulting e.m.f. depend upon the strength and direction of the external field.

The necessary features for a resulting e.m.f. are (i) the time shift in the wave pattern of the induced e.m.f. wave, (ii) the asymmetry of the wave pattern due to hysteresis in the magnetic core. This hysteresis effect gives an e.m.f. curve of small slope on the portion corresponding to the change from the state of saturation toward zero, and of steep slope on the portion corresponding to the attainment of the state of saturation. When two e.m.f.'s in opposition are given a phase shift with respect to each other, the resulting e.m.f. curve is as shown in Fig. 2. It consists of a low voltage peak and a high voltage peak. A circuit with a peak rectified output will then give a d-c. output voltage, the sign and magnitude of which correspond to those of the high peak voltage. The height depends on the amount of the phase shift and hence on the strength of the external field.

Two methods are commonly used for measuring magnetic fields with such transformers. The first is to measure the output of the amplifier, using a proportionality factor between the impressed magnetic field and the output. This method is generally used for measurements on small magnetic fields (0 to 0.1 gauss). The second is to balance out the magnetic field by passing a current through the secondary coils; the current is then an accurate measurement of the magnetic field. This current can be obtained either through manual control or by using feedback from the amplifier itself to drive its output toward zero. In this way higher amplification can be used in the amplifier since its operation is always maintained at the same point in the characteristic.

Measurements can be made with an indicating sensitivity of 1×10^{-5} gauss using equipment of this nature. The accuracy of the measurements is limited chiefly by consistent fluctuations in the earth's field, which average between 2×10^{-5} and 10×10^{-5} gauss, and frequently are as great as 1×10^{-3} gauss. For a detection instrument set in the earth's field, these fluctuations are imposed on the measurements, limiting the readable accuracy.

More accurate measurements of the direction of magnetic fields may be obtained by indicating in directions at right angles to the field. Deviation in position relative to the field then results in an output proportional to the sine of the angle $d\theta$, i.e., $H \sin d\theta \approx Hd\theta$, whereas if measurement is made in the direction of the field the output is proportional to $H \cos d\theta \approx 0$ for small angles.

The Application of Saturated Core Magnetometers to Automatic Steering Controls for Ships

If a magnetometer is suspended with the two magnetic elements horizontal and parallel to each other, but free to rotate together about a vertical axis in the earth's magnetic field, it is evident that the signal output from these coils will vary from zero when the axis of the coils lies along the east-west magnetic line to a maximum when the coils are in the north-south direction. Also the sign of the output will depend upon whether the coils are pointed south or north. Thus the signal resulting from such a pair of coils can be used to control the rudder of a craft in such a way as to keep the axis of the coils in an east-west direction.

Stability equations for the use of such a signal in controlling a ship's steering are derived as follows.

The assumptions upon which this analysis is based are:—

1. The rate of turning of the ship is proportional to the rudder angle

$$P\theta = K_5 M, \tag{5}$$

where P is the operator $\frac{d}{dt}$,

θ is the ship angle,

K_5 is a constant,

M is the rudder angle.

This assumption holds accurately for small, light craft. For the larger sea-going ships there is an additional inertia term which, however, has small effect on the final equations.

2. The output of the amplifier is given by

$$A = \frac{-G(\theta - \theta_0)}{1 + t_2 p}, \tag{6}$$

where G is the amplification factor,

t_2 is the circuit time constant,

$\theta - \theta_0$ is the input signal.

3. The rudder position M may be represented by the equation

$$M = \frac{K_2 A}{L + t_1 p}, \tag{7}$$

where K_2 is a proportionality factor,

A is the amplifier output mentioned above,

t_1 may be regarded as a time constant, depending on the speed of the motor driving the rudder.

These relations may be resolved into a single equation.

$$\left(\frac{t_1 t_2}{K_5} p^3 + \frac{t_1 + t_2}{K_5} p^2 + \frac{p}{K_5}\right) \theta = K_2 G \theta_0 \tag{8}$$

With flux coils held horizontally by gravity loading, there is an added effect on certain courses, as the centrifugal force of the ship's turning gives a false vertical. This may be represented in the amplifier equation:—

$$A \text{ corrected} = \frac{(G(\theta - \theta_0) + K_3 M)}{(1 + t_2 p)}, \tag{6b}$$

where K_3 is a variable, the maximum value of which depends upon the ship's rate of turning and on the value of the vertical component of the earth's magnetic field. It is a maximum for south and north courses and with a positive sign on north course.

The P equation then becomes

$$\left(\frac{t_1 t_2}{K_5} p^3 + \frac{t_1 t_2}{K_5} p^2 + \left(\frac{1}{K_5} - \frac{K_2 K_3}{K_5}\right) p + K_2 G\right) \theta = K_2 G \theta_0, \tag{8b}$$

the positive value of K_3 being used, as the most unstable condition. Stability requires that all the roots of the Equation (8b), with p considered as an algebraic unknown, must have negative real parts.

The effect of this false vertical is thus to decrease the coefficient of the p term on the north courses. The effect can be counteracted by the addition of a feedback of such a nature as to decrease the last term in the equation. Such a feedback was found to be necessary on the first application, a high speed hydrofoil craft, but unnecessary in applications on the larger sea-going types of ships.

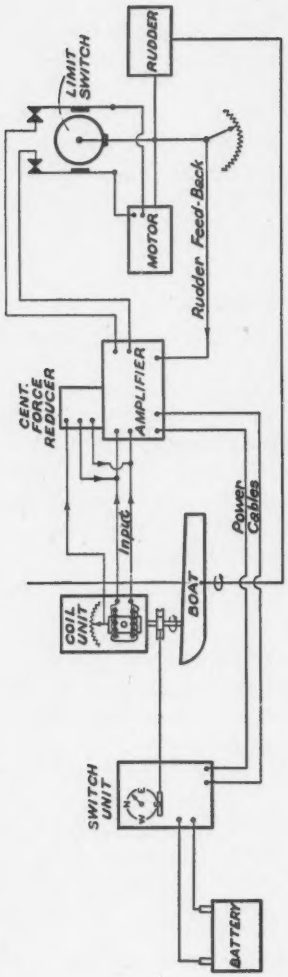

FIG. 3. *Schematic flow diagram.*

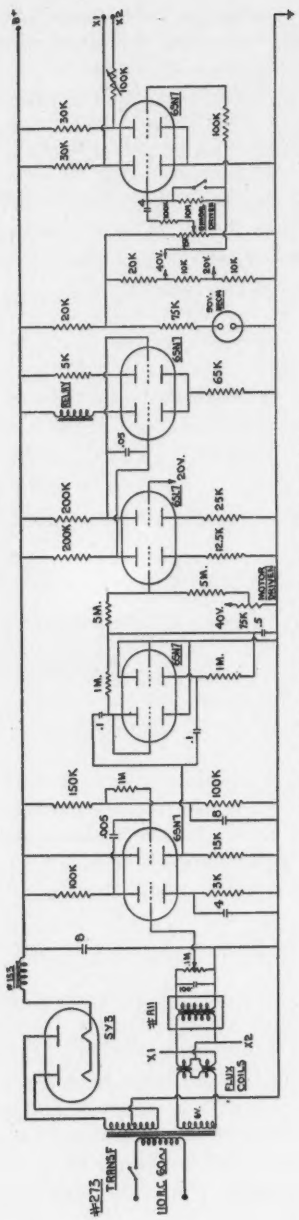

FIG. 4. *Magnetometer steering control amplifier.*

In the mechanism involved in this unit

t_2 is of the order of $\frac{1}{2}$ sec.,

t_1 is widely variable, depending upon the driving motor arrangements ($\frac{1}{2}$ sec. to 1 min.),

K_2 depends upon the effective signal amplification and can be rather widely variable,

K_5 is a constant of the ship being controlled,

K_3 is a constant of any given set of conditions.

An automatic steering control based on these equations was built and trials were made with it in two types of craft, a high speed hydrofoil craft and a Fairmile M.L. ship of the Canadian Navy. The saturated core mode of operation was used because of the simpler design of the amplifier.

Steering Control Equipment

A schematic diagram of the control system is shown in Fig. 3. The essential parts were:

1. The magnetometer coil unit, which consisted of the two gimbal mounted transformers with parallel axes. The axes of the transformers could be fixed at any desired angle with respect to the fore and aft axis of the boat. The transformers were used in the saturated core mode of operation for two reasons. The type of amplifier is smaller and simpler and it was considered that the effect of variations in the magnetic state of the core material could be reduced in this way.

2. The signal from the coil unit was passed, via slip-ring connections, to the amplifier. The wiring diagram is shown in Fig. 4.

3. The output from the amplifier controlled the motor which drove the rudder. The motor drove as well a set of switches which limited its motion to the desired maximum rudder swing. A feedback from the motor output was returned to the amplifier so as to maintain the condition of proportionality between the rudder deflection and input signal.

4. The rudder position caused the boat to turn so that signal from the coils became smaller and the rudder would move toward its zero position.

The gimbal mount must be free to rotate about the axis perpendicular to the boat, so that the pick up coils may be set at any desired angle to the fore and aft axis of the boat. To allow for this rotation it was necessary to use slip rings to carry the signals to and from the coils. An air damping unit to damp out spurious oscillations was incorporated on the gimbal. A sketch of the coil unit, as used in the Fairmile trials, is shown in Fig. 5.

The amplifier used could be powered either by a 6 v. battery vibrator system, or by 110 v. a-c. power, if available. It consisted of a customary a-c. amplification stage, double rectifier, followed by a d-c. amplifier stabilized against variations in the supply voltage. The output of the d-c. amplifier actuated a relay connected to the driving motor.

A potentiometer, driven by the gimbal axis, gave a signal which, after being amplified, fed a current to the secondaries of the transformers so as to compensate for the tilt on the gimbal mount due to centrifugal force developed by the turning of the boat. This signal was coupled so as to decrease to zero with a large time constant (40 sec. was used). Thus the steady state values were maintained at the correct point.

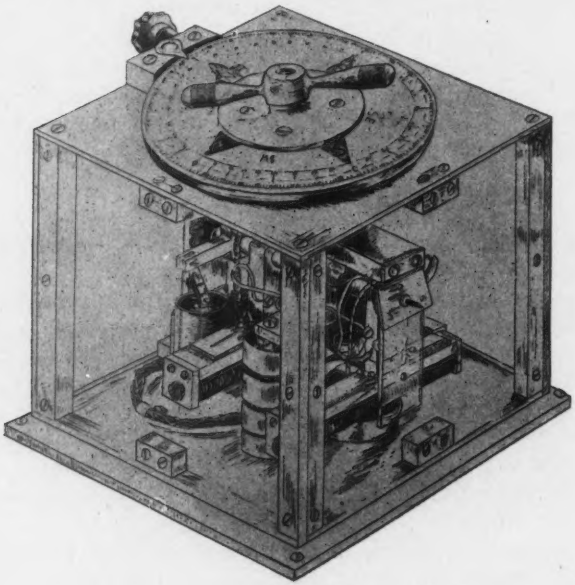

FIG. 5

The driving system maintained a small hunt on the rudder at all times. The magnitude of the hunt was small enough to give no noticeable effect on the course of the ship. In this way, errors due to the finite size of a null point were avoided.

The values of the constants used in the experimental set-up on the Fairmile ship were as follows:—

$$\begin{aligned} t_2 &= \tfrac{1}{2} \text{ sec.} \\ t_1 &= 4 \text{ sec.} \\ K_2K_3 &= \tfrac{1}{3} \text{ sec.} \\ K_5 &= 3/20°/\text{sec./degree} \\ K_2G &= 1. \end{aligned}$$

When these values are substituted in the stability Equation (8), it becomes

$$\left(\frac{40}{3}\,p^3 + \frac{80}{3}\,p^2 + \frac{40}{9}\,p + 1\right)\theta = K_2G\theta_0\,, \qquad (9)$$

and if $\frac{40}{3} p^3 = r^3$, where r is a new operator, the equation becomes

$$(r^3 + 48r^2 + 1.9r + 1)\,\theta = K_2 G \theta_0, \tag{10}$$

which is the equation of a stable system with slight overshoot on changes (2).

The experimental results were satisfactory in both applications of the equipment, the accuracy of steering being $\pm\frac{1}{2}°$ or better. The stability of the control system was in general accord with theoretical expectations, although it was difficult to evaluate exactly and measure the factors involved.

Acknowledgment

The author wishes to acknowledge the assistance of Dr. D. G. Hurst and Mr. J. C. Beynon in designing and testing the equipment, and expresses appreciation to Lt.-Comm. D. Hodgson, R.C.N.V.R., for excellent co-operation in arranging for and assisting in experimental trials.

References

1. Massachusetts Institute of Technology, Department of Electrical Engineering. Magnetic circuits and transformers. John Wiley & Sons, Inc., New York. 1943.
2. Jahnke, E. and Emde, F. Tables of functions with formulae and curves. [Funktionentafeln mit Formeln und Kurven]. Dover Publications, New York. 1943.

THE DIFFUSION LENGTH OF THERMAL NEUTRONS IN HEAVY WATER[1]

By B. W. Sargent,[2] D. V. Booker,[3] P. E. Cavanagh,[3] H. G. Hereward,[3] and N. J. Niemi[4]

Abstract

A continuous flux of thermal neutrons was passed into a large cylindrical tank of heavy water that sat on a graphite column containing a source of photoneutrons. The neutron density in the tank was explored with small indium detectors at selected points along two diameters at right angles in each of three horizontal planes and at 10-cm. intervals along the axis of the tank. The transverse measurements were fitted to Fourier–Bessel series in which the amplitudes of the harmonics were relatively small. The effective radius derived from the transverse analysis was the same in the three planes. The relaxation length of the first component was found from the axial measurements. Corrections were applied for the absorption of neutrons in the axial detector tube, enclosed framework, and indium detectors, and in the light hydrogen in the heavy water. The final value of the diffusion length of thermal neutrons in heavy water (100% D_2O) is 171 $\pm$ 20 cm. Combining this with the known transport mean free path, the capture cross-section is $(0.92 \pm 0.22) \times 10^{-27}$ cm.^{2} per molecule D_2O for neutrons of velocity 2200 m. per second.

Introduction

In the search for a suitable moderator to reduce the non-fission capture of neutrons by uranium and thereby to improve the chances of a chain reaction, the lightest elements were naturally considered. The hydrogenous substances —water and paraffin wax—had already been extensively used to slow down neutrons from laboratory sources. It was recognized, however, that a good moderator for a chain reaction would have to combine good slowing-down properties with small neutron capture. In view of both requirements one of the most promising moderators appeared to be heavy hydrogen or deuterium. It was assumed that the deuterium would be used in the form of heavy water, as the capture cross-section of oxygen was believed to be low. Early experiments designed to measure the capture cross-sections of deuterium and heavy water showed that these were indeed small and consequently difficult to measure. As the result of a series of experiments on uranium compounds and heavy water, the British group became convinced in 1940 that a chain reaction would go. Since 1943 a number of piles containing uranium and heavy water have been built and operated.

If any two of the three related quantities—capture cross-section, transport mean free path, and diffusion length of thermal neutrons in heavy water—are measured experimentally, the third follows. This paper is concerned with the direct measurement of the diffusion length of heavy water, which is one of

[1] *Manuscript received November 30, 1946.*

Contribution from the Nuclear Physics Branch, Montreal Laboratory, Atomic Energy Division of the National Research Council of Canada. Issued as N.R.C. No. 1523.

[2] *Physicist; now at the Chalk River Laboratory.*

[3] *Physicist, United Kingdom Staff.*

[4] *Physicist.*

the nuclear physical quantities required in the design of chain-reacting piles that contain this moderator. Previous attempts to measure directly the diffusion length had indicated that it is very great, and if a reliable estimate were to be obtained a much larger quantity of heavy water than had been used hitherto would be necessary. Last year, when 7600 lb. of heavy water was on hand, the opportunity was presented for such a measurement. This paper contains a brief account* of the method and the final results of the experiment carried out between April 17 and May 12, 1945.

Theory of the Experiment

Suppose that the heavy water is contained in a cylindrical tank on the top of a graphite column and that thermal neutrons are continuously fed into the tank from a source in the graphite. It is convenient to use a system of cylindrical co-ordinates with the origin located near the bottom of the tank and the positive direction of the z-axis vertically upwards along its axis. The radial distance r is measured from this axis, and the angle φ is measured from a vertical plane containing the z-axis.

The diffusion of thermal neutrons may be described by the differential equation

$$\nabla^2\rho - \frac{\rho}{L^2} = 0 \tag{1}$$

in the absence of thermal sources, where ρ is the density of thermal neutrons and L is their diffusion length. Written in cylindrical co-ordinates, Equation (1) becomes:

$$\frac{\partial^2\rho}{\partial r^2} + \frac{1}{r}\frac{\partial\rho}{\partial r} + \frac{1}{r^2}\frac{\partial^2\rho}{\partial\varphi^2} + \frac{\partial^2\rho}{\partial z^2} - \frac{\rho}{L^2} = 0\,. \tag{2}$$

The solution of Equation (2) is required subject to the boundary conditions:

(1) ρ is finite on the axis of the cylinder,

(2) $\rho = 0$ at an effective radius $r = R$ (to be evaluated experimentally),

(3) $\rho = 0$ at $z = h$ (to be evaluated experimentally),

(4) ρ is representable by a measured distribution expressed as a Fourier–Bessel series in the plane $z = 0$.

The desired solution of Equation (2) is

$$\rho = \sum_{\substack{l=0,1,2,\ldots \\ m=1,2,3,\ldots}} (A_{lm}\cos l\varphi + B_{lm}\sin l\varphi)J_l(\lambda_{lm}r)\,\frac{\sinh\dfrac{h-z}{b_{lm}}}{\sinh\dfrac{h}{b_{lm}}}\,, \tag{3}$$

where the relaxation lengths b_{lm} are given by:

$$\frac{1}{b_{lm}^2} = \lambda_{lm}^2 + \frac{1}{L^2}\,. \tag{4}$$

If the experiment is well devised the first term in the Fourier–Bessel Series (3) dominates all others in a large part of the cylinder. In that case the

* *Owing to security restrictions many of the experimental data have been omitted.*

harmonics ($l = 0, m \neq 1$), ($l \neq 0$, any m) are at most small corrections on the dominant term:

$$\rho = A_{01} J_0(\lambda_{01} r) \frac{\sinh \frac{h - z}{b_{01}}}{\sinh \frac{h}{b_{01}}} . \tag{5}$$

In Equation (5)

$$\lambda_{01} = \frac{2.4048}{R} ,$$

and the diffusion length L follows from

$$\frac{1}{L^2} = \frac{1}{b_{01}^2} - \left(\frac{2.4048}{R}\right)^2 . \tag{6}$$

The experimental procedure was to explore the density of thermal neutrons transversely and vertically in the tank. From the transverse analysis the effective radius R of the tank was found, and from the vertical analysis the values of h and b_{01} were derived.

Experimental Details

The experimental tank was made of mild steel with welded seams. The thickness of the wall was 0.4 cm. and that of the bottom and cover 1.1 cm. The inside surfaces were coated with Lithcote enamel to prevent corrosion. The internal radius of the tank was 79.9 $\pm$ 0.3 cm. and the height 165 cm.

The tank containing the heavy water sat on a graphite pedestal having approximately the same shape and diameter as the tank and a height of 28 cm. This pedestal surmounted a rectangular parallelepiped of graphite 279 by 186 cm. in horizontal section and 228 cm. high. When neutrons flow from the parallelepiped of large cross-section into the column of sharply smaller cross-section the harmonics in the density distribution become important. The purpose of the pedestal was to allow the amplitudes of the harmonics to fall off relative to the first component as the neutrons diffuse upwards, and thus simplify the distribution of neutrons across the tank.

The source of neutrons was a block of beryllium at the end of the tube of a General Electric X-ray generator (2) operated at 2000 kv. peak and 1.4 ma. The beryllium was located on the axis of the pile at an average distance of 86 cm. below the centre of the bottom of the tank. This distance was sufficient to ensure that the neutrons entering the tank had reached thermal energies by slowing-down collisions in the graphite. (This point will be examined more closely later.) The exposed surfaces of the graphite pile and tank were covered with cadmium sheet, 0.4 mm. thick, to prevent the escape of thermal neutrons from the system and their entry into the tank after being reflected from the walls of the room.

Indium detectors were used to explore the neutron density in the heavy water. The vertical detector tubes, in which the detectors were placed for activation, were positioned near their lower ends by holes in a horizontal

aluminium grid (3.2 mm. thick) and at their upper ends by holes in the cover of the tank. The grid rested on a narrow flange, tack-welded to the wall of the tank, 8 cm. above the bottom. The detector tubes were made of thin-walled aluminium, and were closed at their lower ends with welded plugs and filled with heavy water to the same level as that in the tank.

The indium foils were 1 cm. square and weighed about 88 mgm. each. These were cemented on aluminium rectangles (2.6 cm. by 2.1 cm. by 0.53 mm.) for convenience in handling. The detectors were positioned on light aluminium frameworks and lowered into the detector tubes. Vertical measurements on the detectors were made with a cathetometer, and radial distances were determined by the holes in the aluminium grid and cover of the tank. Similar indium foils were used to monitor the output of the source of neutrons and were placed for activation at a standard position 126 cm. below the middle of the beryllium block in the graphite parallelepiped. The foils activated in the tank were counted against the corresponding monitoring foil. The half-period of indium activity was taken to be 54.5 min., as measured in this laboratory. The relative sensitivities of the detectors were measured and taken into account. The geometry at the Geiger–Müller counters was accurately reproducible, and the behaviour of the counters, high tension supplies, and scales-of-128 was very satisfactory. The initial counting rate of the monitors was approximately 2500 β-particles per minute after the X-ray generator had been operated at full voltage and current for 1.5 hr. The corresponding rate for a foil activated at the lowest point selected in the tank was 2175 β-particles per minute.

The experiment was performed with two different quantities of heavy water. When 5800 lb. of heavy water was in the tank the neutron density was measured at approximately 10-cm. intervals along the axis of the tank and at selected points along two diameters at right angles in three approximately horizontal planes spaced at 20 and 30-cm. intervals. Six indium detectors were used in each run, three being in one detector tube and three in another. The two detector tubes were usually kept 50 cm. or more apart to avoid any influence of the neutron capture by one tube on the neutron density being measured in the other. The indium foils in a given tube were spaced at 20-cm. intervals to reduce to a negligible amount (estimated at 0.03%) the influence of one foil on the activity acquired by another. The density of neutrons at each point on the axis was measured six to ten times and at the other points four times. In half of the runs the indium foils faced the axis of the tank, and in the other half they faced the wall. The slight dependence of the activity on the neutron current drops out in the average, which is a measure of the neutron density.

When the supply of heavy water was increased to 7600 lb. some of the measurements were repeated. The neutron density was measured at approximately 10-cm. intervals along the axis of the tank using six indium foils spaced at 20-cm. intervals in a given run. Each point was measured six

times. The agreement obtained in the various runs was satisfactory, the probable error in the mean being about ½% for all except a few points where the neutron density was low.

Experimental Results

Two minor corrections were applied to the averaged density measurements at the various points.

(1) While the vertical positioning of the detectors in the tank was measured to 0.1 mm., it was impracticable to obtain better reproducibility of vertical positioning in different runs than ±5 mm. Consequently, the variations $\triangle z$ of points from the horizontal planes chosen at $z = 0$, 20.00, and 50.00 cm. were allowed for. The corrections to ρ were based on the assumption of a single term for the neutron density:

$$\rho = A_{01}J_0(\lambda_{01}r)\,\frac{\sinh\dfrac{h-z}{b_{01}}}{\sinh\dfrac{h}{b_{01}}}\,, \tag{5}$$

from which

$$\frac{\triangle\rho}{\rho} = -\frac{\triangle z}{b_{01}}\coth\frac{h-z}{b_{01}} \tag{7}$$

with sufficient accuracy. ($\triangle z$ was always less than 1 cm.)

(2) Though the detector tubes were straight, they were not exactly parallel to the vertical axis of the tank. The radial distances measured at the grid and just above the cover (160 cm. above the grid) did not differ by more than 5 mm., and the former set was adopted as standard. The correction to ρ for a departure $\triangle r$ from a standard distance r was taken to be:

$$\frac{\triangle\rho}{\rho} = -\lambda_{01}\triangle r\,\frac{J_1(\lambda_{01}r)}{J_0(\lambda_{01}r)}\,. \tag{8}$$

Approximate values of b_{01}, h and R (hence λ_{01}) were sufficient for these two corrections.

The measurements of the neutron density were analysed according to the Distribution (3), which was derived as the solution of the diffusion Equation (1) in which the thermal source term was set equal to zero. The validity of this assumption will now be considered. If the threshold for the photodisintegration of the beryllium nucleus is 1.63 Mev. the *maximum* energy of the photoneutrons is 330 kev. when the X-ray generator is operated at 2.0 Mv. peak. According to the calculations of Marshak (5), the slowing-down length from this initial energy to thermal energies is about 16.3 cm. in graphite (density 1.6 gm. per cc.). It can be shown from slowing-down and diffusion theory that the fraction of epithermal neutrons is very small and their effect on the thermal distribution negligible after the neutrons have traversed 86 cm. of graphite (5.3 slowing-down lengths) between the middle of the beryllium block and the bottom of the tank. In addition, the neutrons had to traverse 6.4 cm. of heavy water to reach the lowest point in the tank

at which their density was measured, and thus they suffered further slowing-down collisions. The sources of thermal neutrons within the volume of heavy water actually used for measurements may therefore be neglected. Moreover, the activity acquired by absorption of neutrons of resonance energy (1.44 ev. (4)) in the indium foils may also be neglected. This latter point was substantiated by a few measurements with indium foils shielded by 1 mm. of cadmium.

The transverse measurements in the plane $z = 0$ were first examined graphically, and the symmetrical part of the density was found to be well represented by

$$A_{01}J_0(\lambda_{01}r) + A_{02}J_0(\lambda_{02}r) + A_{03}J_0(\lambda_{03}r), \tag{9}$$

where $A_{02}/A_{01} = 2\%$ and $A_{03}/A_{01} = 1\%$. Secondly, the relaxation lengths b_{02} and b_{03} were estimated from Equation (4) using approximate values of L and R; and the contributions of these two harmonics were calculated and subtracted from the measured densities in the planes $z = 0$, 20.00, and 50.00 cm. Thirdly, the remainders were fitted by the method of least squares to the expression:

$$\rho = A'_{01}(z)J_0(\lambda_{01}r) + (A'_{11}(z)\cos\varphi + B'_{11}(z)\sin\varphi)J_1(\lambda_{11}r), \tag{10}$$

yielding the values of the amplitudes and effective radius R of the tank in each of the three planes. Details are as follows. Since the amplitudes $A'_{11}(z)$ nd $B'_{11}(z)$ are small in comparison with $A'_{01}(z)$ and the effective radius is close to 82.8 cm., we set

$$\lambda_{11} = \frac{3.8317}{82.8}\ \text{cm.}^{-1}.$$

The variables that remain to be determined are $A'_{01}(z)$, $A'_{11}(z)$, $B'_{11}(z)$ and λ_{01} (or R). $J_0(\lambda_{01}r)$ is expanded to two terms in a Taylor's series about $\lambda'_{01}r$, where

$$\lambda'_{01} = \frac{2.4048}{82.8}\ \text{cm.}^{-1}.$$

Equation (10) becomes:

$$\rho = A'_{01}(z)J_0(\lambda'_{01}r) + A'_{01}(z)\frac{\delta R}{R}\lambda'_{01}rJ_1(\lambda'_{01}r) + (A'_{11}(z)\cos\varphi + B'_{11}(z)\sin\varphi)J_1(\lambda_{11}r). \tag{11}$$

It is convenient to regard $A'_{01}(z)$, $A'_{01}(z)\frac{\delta R}{R}$, $A'_{11}(z)$, and $B'_{11}(z)$ as independent variables, for the normal equations derived from the application of the method of least squares to the experimental equations are then linear. In the plane $z = 0$, $A_{11}/A_{01} = 7.4\%$ and $B_{11}/A_{01} = 7.2\%$. The effective radius R is given in Table I.

The effective radius is therefore $82.56 - 79.9 = 2.66$ cm. greater than the average internal radius of the steel tank tightly wrapped on the outside with cadmium. Auger, Munn, and Pontecorvo (1) determined the extrapolated cut-off distance to be 1.64 cm. from the curve of the density of thermal neutrons in heavy water below a flat cadmium plate. Since the

effect of the small curvature of the tank is believed to be negligible, the whole difference 1.0 cm. is attributed to the neutron scattering by the steel wall of thickness 0.4 cm.

TABLE I

z, cm.	R, cm.
0	82.56
20	82.47
50	82.65
	Average 82.56

An approximate value of the relaxation length b_{01} was obtained from the sets of densities measured at the same r and φ in the three planes. After these densities had been corrected for the harmonics $J_0(\lambda_{02}r)$, $J_0(\lambda_{03}r)$ and $J_1(\lambda_{11}r)$ they were substituted into Formula (5):

$$\rho = A''_{01}(r) \frac{\sinh \frac{h-z}{b_{01}}}{\sinh \frac{h}{b_{01}}}. \tag{5a}$$

A more accurate value of the relaxation length b_{11} was found from the two sets of measurements at 10-cm. intervals along the axis of the tank. First, these were corrected for the harmonics $J_0(\lambda_{02}r)$ and $J_0(\lambda_{03}r)$, using the amplitudes found in the transverse analysis for $z = 0$ and the estimated relaxation lengths. Second, the vertical distance h from the chosen origin to the horizontal plane at which the neutron density vanishes was estimated from the second set of measurements at points nearest this plane. As a first approximation this plane was assumed to be 3 cm. above the surface of the heavy water. Therefore

$$\rho = \left(A_{01}/\sinh \frac{h}{b_{01}}\right) \sinh \left(\frac{h' + \delta - z}{b_{01}}\right), \tag{5b}$$

where δ is the correction to the first approximation h', and b_{01} is approximately known. The densities ρ measured at three points, four points, etc., to seven points, counting downward from the plane of vanishing density, were used in turn in this expression and δ found by the method of least squares. The final result was $\delta = -0.1 \pm 0.1$ cm. Third, using the appropriate value of h, the relaxation length b_{01} was derived from each set of axial measurements. The densities ρ (corrected for the harmonics) should be represented by:

$$\rho = A_{01} \frac{\sinh \frac{h-z}{b_{01}}}{\sinh \frac{h}{b_{01}}}, \tag{5}$$

which may be rewritten:

$$\rho = A_{01} e^{-z/b_{01}} \left(\frac{1 - e^{-2(h-z)/b_{01}}}{1 - e^{-2h/b_{01}}}\right). \tag{5c}$$

The last factor may be regarded as the end-correction for the finite length of the column of heavy water. It was evaluated for h and a likely value of b_{01} and applied as a correction to ρ. The method of least squares was then applied to the logarithms of the ρ's (so corrected) to yield b_{11}. If we write b_{01} (assumed) for the value substituted in the end-correction, and b_{01} (derived) for the value derived from the least squares solution, it is found that b_{01} (derived) varies linearly with b_{01} (assumed). This is a useful property in arriving at the final result, at which b_{01} (derived) = b_{01} (assumed).

Up to this point we have neglected the effect of the neutron capture by the axial detector tube, enclosed framework, and indium detectors. The diffusion theory was applied to give the necessary correction (+ 2%) to the diffusion length derived from Equation (6).

Finally, the diffusion length, measured in the heavy water of known isotopic composition, was corrected for the neutron capture in the light hydrogen present to yield the diffusion length in pure heavy water (100% D_2O).

The capture cross-section of hydrogen was derived from the following measurements. Whitehouse and Graham (8) have found

$$\sigma_B/\sigma_H = 2270$$

in a series of careful measurements. The $1/v$ law of neutron capture by boron has been well substantiated by Rainwater and Havens (7). From work at the Argonne Laboratory (3, 6)

$$\sigma_B = 705 \times 10^{-24} \text{ cm.}^2\text{/atom}$$

for neutrons of velocity 2200 m. per sec. From these data

$$\sigma_H = 0.273 \times 10^{-24} \text{ cm.}^2\text{/atom}$$

for neutrons of velocity 2500 m. per second.

The diffusion length L is related to the transport mean free path l_t and the mean free path for capture l_c by the diffusion formula:

$$L^2 = \frac{1}{3} l_t l_c . \tag{12}$$

where $l_c = v\tau$, τ being the mean lifetime of thermal neutrons in heavy water and v their average velocity (2500 m. per sec.) at room temperature. Setting $l_t = 2.4 \pm 0.1$ cm., as measured by Auger, Munn, and Pontecorvo (1), and correcting for neutron capture in the light hydrogen present, we find that

$$L = 171 \pm 20 \text{ cm.}$$

in heavy water of 100% purity, and that the capture cross-section is $(0.81 \pm 0.19) \times 10^{-27}$ cm.^{2} per molecule D_2O for neutrons of velocity 2500 m. per second. Assuming a $1/v$ law of capture,

$$\sigma_c = (0.92 \pm 0.22) \times 10^{-27} \text{ cm.}^2\text{/molecule } D_2O$$

for neutrons of standard velocity 2200 m. per second.

Acknowledgments

The Geiger–Müller counters were made for us by Mr. N. Veall, and the stabilized high tension supplies and scales-of-128 by Mr. H. F. Freundlich and staff. Mr. F. W. Fenning made the indium detectors and devised the detector holders that fitted over the Geiger–Müller counters in the course of some earlier experiments in which he collaborated with us. We are grateful for their assistance.

We should also like to thank Miss E. O'Brien for operating the X-ray generator and Miss Y. Diamond, Miss G. Despins, Mrs. S. Courant, and Miss H. Zackon for counting.

References

1. AUGER, P., MUNN, A. M., and PONTECORVO, B. Can. J. Research, A, 25 : 143-156. 1947.
2. CHARLTON, E. E. and WESTENDORP, W. F. Electronics, 17(12) : 128-133. 1944.
3. FERMI, E. Private communication. 1944.
4. HAVENS, W. W., JR. and RAINWATER, J. Phys. Rev. 70 : 154-173. 1946.
5. MARSHAK, R. E. Unpublished report, MT-18. On the moments of the distribution function of neutrons slowed down in heavy elements. National Research Council of Canada. 1943.
6. MARSHALL, J. Bull. Am. Phys. Soc. 21(3) : 12, F4. 1946.
7. RAINWATER, J. and HAVENS, W. W., JR. Phys. Rev. 70 : 136-153. 1946.
8. WHITEHOUSE, W. J. and GRAHAM, G. A. R. Unpublished report, MP-172. The ratio of the neutron absorption cross-sections of boron and hydrogen. National Research Council of Canada. 1945.

THE TRANSPORT MEAN FREE PATH OF THERMAL NEUTRONS IN HEAVY WATER[1]

BY P. AUGER,[2] A. M. MUNN,[3] AND B. PONTECORVO[4]

Abstract

The transport mean free path of thermal neutrons in heavy water is determined from measurements of the neutron density in heavy water (99.4 atoms of deuterium per 100 atoms of hydrogen element) at various distances from a cadmium plate. In the region investigated, the density is found to be a linear function of the distance from the cadmium plate. When this straight line is extrapolated, the density vanishes at a distance $d = 1.64$ cm. behind the plate. On the basis of transport theory it is known that $d = 0.71 l_t$, where l_t is the transport mean free path in the medium. The final result is $l_t = 2.4$ cm. in pure heavy water. The measurements of the neutron density show that it falls below the straight line as the cadmium surface is very closely approached, in agreement with transport theory.

Introduction

Let $l(v)$ be the scattering mean free path in a medium for neutrons of velocity v. The corresponding transport mean free path, $l_t(v)$, is defined by the relation

$$l_t(v) = \frac{l(v)}{1 - (\cos\theta)_{av}}, \tag{1}$$

where $(\cos\theta)_{av}$, the mean cosine of the scattering angle θ in single collisions, represents quantitatively the amount of coherence between two successive free paths in the medium considered. From the Definition (1) it is recognized that the transport mean free path, rather than the scattering mean free path, enters fundamentally in problems of neutron diffusion. When the scattering is isotropic, l_t is equal to l.

It should be noticed that the scattering mean free path and, consequently, the transport mean free path, may vary considerably with the neutron velocity in the *thermal region*. In the case of crystalline matter, for example, only the mean free path of monokinetic neutrons, impinging upon the crystal at a given incidence, is a well defined quantity, while the notion of mean free path (and of transport mean free path) of *thermal neutrons* has not a precise meaning. One should expect to find different results according to the various experimental conditions affecting the mean neutron velocity. In a liquid like heavy water, however, rapid variations of the scattering cross-section with the neutron energy within the thermal region are hardly expected, and the notion of transport mean free path of thermal neutrons has a definite meaning.

[1] *Manuscript received September 17, 1946.*

Contribution from the Montreal Laboratory, Nuclear Physics Branch, Division of Atomic Energy, National Research Council. (Work performed in 1943.) Issued as N.R.C. No. 1524.

[2] *Member of the United Kingdom staff; now at the Ecole Normale Supérieure, Paris, France.*

[3] *Junior Research Physicist, National Research Council; now at McGill University, Montreal, Que.*

[4] *Member of the United Kingdom staff; now at the Chalk River Laboratory, Chalk River, Ontario.*

One should accordingly get the same value of l_t for thermal neutrons in heavy water by changing the experimental conditions, thus slightly affecting the mean neutron velocity. In all considerations below it will be tacitly assumed that all the thermal neutrons have the same velocity v equal to their average velocity.

Purpose of the Experiment

The experiment described in this paper was performed because with the knowledge of l_t the following information pertaining to heavy water can be derived.

(1) The value of the capture mean free path l_c of thermal neutrons can be derived from the well known relation of diffusion theory:

$$L^2 = \frac{1}{3} l_t l_c , \tag{2}$$

where L, the diffusion length of thermal neutrons in the medium, is known from a separate experiment. Conversely, the value of L can be derived when l_t and l_c are known.

(2) The correct boundary condition* for the neutron density can be written in problems concerning the diffusion of neutrons. Examples are experiments designed to measure diffusion lengths, exponential experiments with multiplying media, and technical problems concerning reflectors for chain reacting piles and concerning thermal utilization of neutrons in heterogeneous chain reacting systems.

(3) The value of $(\cos \theta)_{av}$ can be derived from Equation (1). This is an interesting quantity, characteristic of the scattering of thermal neutrons in heavy water.

Methods That May Be Used for Determining l_t

Since l_t and l are not expected to differ much in value, an experimental measurement of l_t will definitely distinguish it from l only if the method is capable of good accuracy, say to 5%. This consideration and the fact that only 13 litres of heavy water was available have been weighed in selecting the experimental method from the five described below.

(1) The study of the angular distribution of thermal neutrons after single collisions in heavy water provides a direct method of measuring $(\cos \theta)_{av}$ and consequently, by Equation (1), the transport mean free path. The neutron sources available were not sufficiently strong to provide the extremely intense and well collimated beam of thermal neutrons that this method requires.

(2) If the diffusion length L and the mean lifetime τ of thermal neutrons in a heavy water medium are known from experiments, the diffusion coefficient D can be deduced from the diffusion Relation (2), which may be written:

$$L^2 = D\tau = \frac{1}{3} l_t v \tau. \tag{3}$$

* *This will be explained later.*

The diffusion length of thermal neutrons in heavy water is so great that it cannot be measured when only a quantity of the order of 100 litres is available. Hereward, Laurence, Munn, Paneth, and Sargent (6) have, however, measured the diffusion length in heavy water containing lithium carbonate. The neutron capture by the lithium reduced the diffusion length to such a value that it could be measured in a quantity of the order of 100 litres. Since the mean free path is not appreciably changed by the addition of lithium carbonate, the diffusion coefficient D follows from Equation (3) when L and τ are substituted. For this purpose τ would be estimated from the known capture cross-sections and numbers of atoms per cubic centimetre of the constituents. It should be noticed that this method yields directly the diffusion coefficient, and the transport mean free path follows only after a value of the neutron velocity v is assumed. In spite of the uncertainty in the neutron velocity that is appropriate, the value of l_t obtained in the present experiment and the values of L and τ in Reference (6) satisfy Equation (3) fairly well.

(3) Suppose that a thermal neutron detector, geometrically thin but infinitely thick with respect to thermal neutrons, is placed deep within the scattering medium with its faces normal to the gradient of the neutron density. If the area of the detector is so small that the neutron field is not modified, it can be shown that the sum S of the β-activities, I_1 and I_2, of the two faces is proportional to the neutron density ρ, while the difference Δ, $I_1 - I_2$, is proportional to the neutron current density j:

$$S = I_1 + I_2 = \tfrac{1}{2}k\rho v \tag{4}$$

$$\Delta = I_1 - I_2 = kj. \tag{5}$$

The constant k of proportionality is the same in the two equations except for a small correction that arises from the fact that the neutrons impinging on the two sides of the detector have slightly different angular distributions. When Equations (4) and (5) are combined with the expression for the current density in diffusion theory:

$$j = -D \operatorname{grad} \rho = -\frac{1}{3} l_t v \operatorname{grad} \rho, \tag{6}$$

it follows that

$$\Delta = -\frac{2}{3} l_t \operatorname{grad} S. \tag{7}$$

This experimental method of measuring l_t therefore consists of measuring the difference of the β-activities of the two faces and the gradient of their sum and using Equation (7).

It is not possible to use an infinitely thick detector, but a moderately thick detector of small area backed by a (strongly absorbing) cadmium sheet of the same area would meet the requirements. This method was not used because, with the neutron sources available, the β-activities were too small for measurement when the linear dimensions of the detector were a small fraction of the scattering mean free path in the medium.

(4) Suppose that the scattering medium is bounded by a plane surface, which is a perfectly absorbing sheet or a boundary to vacuum. If ρ_s represents the density of thermal neutrons and j_s the current density, both at the surface, on the basis of an isotropic scattering law it follows exactly (11) that

$$\rho_s = \sqrt{3} j_s / v. \tag{8}$$

If the scattering law is more complicated, Equation (8) is a good approximation (8).

Owing to continuity, j_s is approximately equal to the current density at points distant a few scattering mean free paths from the boundary. At this depth, however, diffusion theory is valid and Equation (6) can be applied. Therefore

$$j_s = v\rho_s/\sqrt{3} = -\frac{1}{3} l_t v \operatorname{grad} \rho,$$

or

$$l_t = -\sqrt{3}\,\rho_s / \operatorname{grad} \rho, \tag{9}$$

where grad ρ stands for the gradient of the density at a point close to the boundary, but far enough from it to permit the use of diffusion theory.

While in principle this method is simple and very accurate, in practice a serious difficulty arises. An extremely thin detector of neutrons is required, since the neutron density must be measured within the medium where the distribution of neutron velocities is almost isotropic and also at the boundary where the distribution is very anisotropic.

(5) The principle of this method, which was adopted for measuring l_t in heavy water, had been used before by Amaldi and Fermi (1) in their work on the motion of neutrons in hydrogenous materials. The theory will be presented in detail in the next section. It will be seen later that this method possesses some practical advantages.

Principle of the Method Selected for Determining l_t in Heavy Water

Suppose that a plane source of thermal neutrons at infinity produces a stream of neutrons of velocity v in a semi-infinite scattering medium, limited to the right at $z = 0$ by a perfectly absorbing sheet or a vacuum. If no capture of neutrons takes place in the medium the current density j is constant everywhere. In regions far from the boundary (a few mean free paths) diffusion theory may be applied. Under these assumptions it can easily be shown that the neutron density $\rho(z)$ is a linear function of z. Near the boundary, however, only transport considerations may be applied. It has been shown theoretically that $\rho(z)$ falls below the straight line near the boundary and its gradient becomes infinite there (10, 11). If the straight line is extrapolated outside the medium the density vanishes at a certain distance from the boundary. This distance d is related to l_t by a numerical relation, obtained by Placzek and collaborators (8-11), which is known to good accuracy as stated below.

Let the scattering law be represented by the function $f(\cos\theta)$ such that $f(\cos\theta)\, d(\cos\theta)$ is the probability that the cosine of the scattering angle θ in one collision lies between $\cos\theta$ and $\cos\theta + d(\cos\theta)$. By definition,

$$\int_{-1}^{1} f(\cos\theta)\, d(\cos\theta) = 1 \tag{10}$$

and

$$(\cos\theta)_{av} = \int_{-1}^{1} \cos\theta\, f(\cos\theta)\, d(\cos\theta). \tag{11}$$

If $f(\cos\theta)$ is expanded in terms of Legendre polynomials $P_l(\cos\theta)$,

$$\begin{aligned} f(\cos\theta) &= A_0 + A_1 P_1(\cos\theta) + A_2 P_2(\cos\theta) + \cdots \\ &= A_0 + A_1\cos\theta + \tfrac{1}{2}A_2(3\cos^2\theta - 1) + \cdots, \end{aligned} \tag{12}$$

the coefficients A_0 and A_1 are derived by substituting Equation (12) in Equations (10) and (11) respectively and carrying out the integrations. Equation (12) can therefore be written:

$$f(\cos\theta) = \tfrac{1}{2}[1 + 3(\cos\theta)_{av}\cos\theta + A_2(3\cos^2\theta - 1) + \cdots]. \tag{13}$$

The relation between d and l_t for several scattering laws has been investigated by Mark (9). When the scattering is isotropic ($f = \frac{1}{2}$ and $l = l_t$), the relation, according to Placzek and Seidel (11), is

$$d = 0.71\, l. \tag{14}$$

When the scattering law is represented by

$$f(\cos\theta) = \tfrac{1}{2}[1 + 3(\cos\theta)_{av}\cos\theta]$$

Mark shows that

$$d = 0.71\, l_t. \tag{15}$$

When the next Legendre polynomial is included in the scattering law,

$$f(\cos\theta) = \tfrac{1}{2}[1 + 3(\cos\theta)_{av}\cos\theta + A_2(3\cos^2\theta - 1)],$$

Mark obtains

$$d = 0.71 l_t[1 + a(A_2)] \tag{16}$$

with $a(A_2) < 0.005$.*

From a comparison of Expressions (14), (15), and (16), it is reasonable to assume that even for a scattering law in which higher moments of the angular distribution function are not negligible, d is not very different from (15).

Fermi's relation (4),

$$d = l/\sqrt{3} = 0.58l, \tag{17}$$

which was used in the original work of Amaldi and Fermi (1) with paraffin, is not accurate, although the original law for the angular distribution of neutrons emerging from a plane surface,

$$\cos\theta + \sqrt{3}\cos^2\theta,$$

is a very good approximation, as shown by Placzek (10).

** It is easy to see that there is a limitation to the value of A_2, for $f(\cos\theta)$ must be greater or equal to zero. The value of $a = 0.005$ holds for the maximum value of A_2.*

In the experimental method adopted for determining l_t, the density of thermal neutrons is measured at various distances from a plane boundary but in the region where diffusion theory is applicable. The measured distribution is extrapolated to the point of zero density, which determines d and in turn l_t from Equation (15). Since the detector of thermal neutrons is not to be used close to the boundary, the requirements of its properties are less severe than in Method (4). A small boron trifluoride chamber, having the practical advantage of almost zero background, may be used in spite of the fact that its presence makes a sizable hole in the medium.

In order to simulate the ideal conditions described in presenting the principle of the method, the following conditions must be fulfilled.

(1) There must be no sources of thermal neutrons in the heavy water.

(2) The boundary of the heavy water must be plane and sharply defined. (There must be no back scattering.)

(3) In the region where density measurements are made $\rho(z)$ must be a linear function of z to an accuracy such that the departure from linearity is smaller than the experimental error.

Condition (1) was fulfilled by placing the source of fast neutrons in a graphite pile at a distance from the tank of heavy water so great that epithermal neutrons were practically non-existent in the heavy water (13, pp. 55–56, para. 4.2 and 4.6 (*a*)). Condition (2) was fulfilled by defining the heavy water boundary with a thick cadmium plate. Since the capture mean free path in cadmium is of the order of 0.1 mm., practically no neutrons are reflected. Condition (3) is fulfilled if the relaxation length L_r of the pile is sufficiently great. At large distances from the source, the density of thermal neutrons in the graphite is given by

$$\rho(z) = A \sinh \frac{z+d}{L_r} = A\left(\frac{z+d}{L_r}\right)\left[1 + \frac{1}{6}\left(\frac{z+d}{L_r}\right)^2 + \cdots\right], \quad (18)$$

where A is a constant and z is measured from the plane boundary.* The term that represents the first order departure of $\rho(z)$ from linearity, $\frac{1}{6}[(z+d)/L_r]^2$, is sufficiently small if L_r is sufficiently large.

Since the relaxation length L_r of thermal neutrons in a square pile of moderator can be related (see for example Reference (7)) to the diffusion length L and the side length a of the pile:

$$\frac{1}{L_r^2} = \frac{1}{L^2} + \frac{2\pi^2}{a^2}, \quad (19)$$

a large value of L_r is obtained when a is large, i.e., when the loss of neutrons through the sides is small. Since only 13 litres of heavy water was available, it was necessary to reduce the leakage of neutrons through the sides of the tank by an artificial means. This was accomplished by embedding the tank in the

* *Equation (18) may be regarded as a definition of the relaxation length L_r of neutrons in the graphite pile.*

graphite (Fig. 1). In this way the escape of neutrons through the sides of the tank is essentially determined by the dimension a of the graphite pile. Since the diffusion length of thermal neutrons in heavy water is greater than in graphite, the relaxation length in the heavy water is at least as great as in the graphite pile with graphite replacing the heavy water. Setting $L = 51$ cm. and $a = 190$ cm. in Equation (19), $L_r = 33$ cm. for thermal neutrons in this graphite pile. It is necessary, however, that the radius of the tank be large in comparison with the transport mean free path in heavy water.

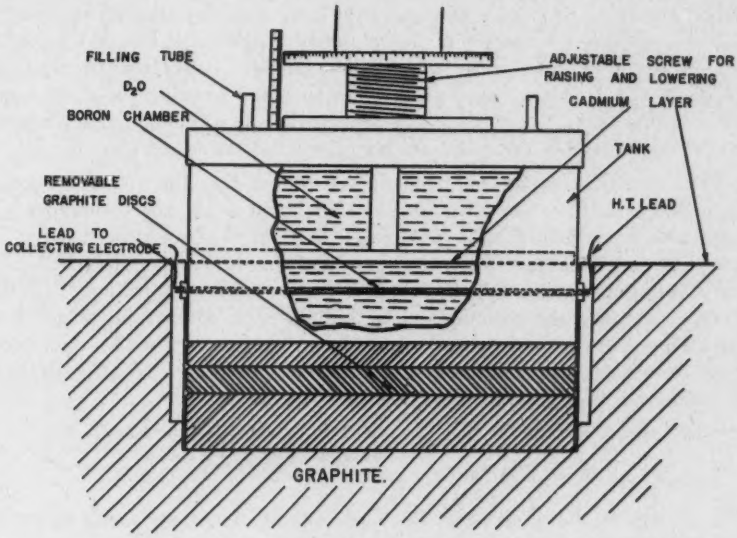

FIG. 1. *Experimental arrangement.*

Experimental Arrangement

The experimental arrangement is shown in Fig. 1. The graphite pile was 250 cm. high and of square cross-section, 188 cm. on the side.

The source of neutrons was 2.4 gm. of radium mixed with beryllium. It was placed on the vertical axis of the pile 97 cm. below the top of the graphite and hence 97 cm. below the heavy water boundary. In one experiment, however, the source was placed 132 cm. below the common boundary. The upper surface of the pile was covered with cadmium sheet approximately 1 mm. thick.

The aluminium tank containing 11.32 kgm. of heavy water had an internal diameter of 29.9 cm., a wall thickness of 1.5 mm., and a height of 16 cm. The aluminium lid was sealed in place with wax. The rod used to raise and lower the cadmium plate passed through a central hole in the lid, which was made air-tight with a rubber gasket. An aluminium tube, 6.35 mm. in

outside diameter, and of wall thickness 0.85 mm., crossed the tank along a diameter 4.45 cm. above the bottom. This tube housed a boron trifluoride chamber, 4 mm. in outside diameter, at its middle point.

The heavy water boundary was defined by the lower surface of a cadmium layer, 1 mm. in thickness, sprayed on a horizontal steel disk, 8 mm. thick, which was fixed to the vertical rod. By means of the micrometer screw the disk could be moved over a distance of 9 cm.

In order to vary the distance of the chamber from the cadmium surface and at the same time keep the cadmium level with the graphite surface, the disk was displaced by means of the micrometer screw and the tank raised or lowered to compensate for the former displacement. Graphite disks of graded thicknesses, 1, 2, 5 cm., were used under the tank to bring about the necessary compensation. In this way the neutron density was explored at a number of distances between the cadmium boundary and the boron chamber.

The alternative to the method adopted for varying the distance between the chamber and boundary would have been to move the boron chamber with respect to a stationary cadmium plate. The method adopted has the following advantages. (1) The very fragile chamber remains undisturbed inside the aluminium tube, and hence there is little chance of breakage. (2) The distance between the cadmium plate and the aluminium tube, which is an essential parameter in the measurements, can be measured with a micrometer screw to a high degree of accuracy. It is safe to state that the distance a of the tube from the plate was known to ± 0.1 mm.

The distance z from the plate to the chamber was taken to be

$$z = a + \text{half the outer diameter of the tube.}$$

The possibility that errors arise in this procedure, and experiments to test the validity of the procedure, will be discussed later.

The interior of the tank and the other surfaces in contact with the heavy water had been painted with a zinc chromate primer to protect the metals against corrosion. The thickness of this coat on the cadmium was such a small fraction of the scattering mean free path in the primer that its presence introduced no error. No corrosion of the cadmium took place for no drift in the counting rate of the chamber was observed (at a given position) over a period of three weeks.

During the series of measurements the temperature of the heavy water was fairly constant at 22° C.

Neutron Detector

For the measurement of neutron densities a boron trifluoride chamber was chosen in preference to a detector having the property of becoming radioactive under neutron bombardment for the following reasons.

(1) For a given neutron absorption a boron trifluoride chamber has a greater efficiency (number of pulses counted per neutron absorbed) than any

detector having the property of becoming β-active. Moreover, there is some practical advantage in being able to count in the presence of the source.

(2) For the low counting rates that are encountered in this experiment, the fact that the chamber has practically no background is a great advantage. The background of the chambers used was about one count per hour. Moreover, the neutron counting rates do not drift over long periods of time.

(3) Although the boron trifluoride chamber has dimensions that cannot be reduced beyond a certain practical limit, *relative* measurements of neutron density can be made without error in the present experiment where the density is a linear function of z. Under this condition, in fact, the counting rate is altered through the finite dimensions of the chamber by a factor that is independent of z. The z-co-ordinate defining the position of the chamber can be identified as that of its geometrical centre, provided that the symmetry about the axis of the chamber is perfect. It will be shown that this requirement was met.

The boron trifluoride chambers, one of which is shown in Fig. 2, were of a series made by Mr. N. Veall (14). They were filled with boron trifluoride to a pressure of 2 atm. The cathode, anode, and guard-ring were made of platinum. The collecting voltage was 600 in most of the experiments.

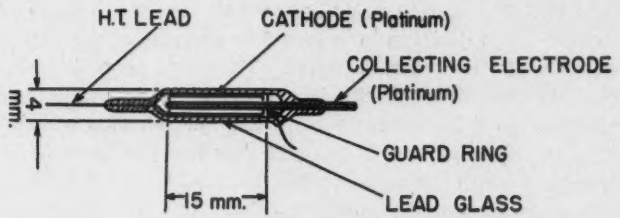

FIG. 2. *Boron trifluoride chamber.*

The chamber was connected to a linear amplifier of conventional design, the first tube of which was situated as close as possible to the chamber. The amplifier was followed by a discriminator, to reject pulses smaller than a chosen size, and a scale-of-32. Counting rates were reproducible within the statistical accuracy during the whole series of measurements, which lasted one month.

In order to estimate the neutron absorption in the chamber as a whole, the lead glass (Corning G-12) used to make the envelope was analysed. Taking the known capture cross-sections and numbers of nuclei in the constituents (boron, fluorine, oxygen, aluminium, silicon, sodium, potassium, lead, and platinum) of the chamber and an equal length of the enclosing aluminium tube, the chamber was found to be equivalent in absorption to about 1 mgm. of boron.

The error arising from the perturbation of the neutron density by the detector must be estimated because this perturbation would cause the density to be underestimated by a factor that is larger the farther the detector is from the boundary. Consequently the measured cut-off distance d would be too great, if the error under consideration were not negligible. The following considerations show, however, that the detector was so thin with respect to neutron capture that its perturbation introduces negligible errors in comparison with the statistical errors. For convenience, the actual case is reduced to simple geometry by supposing that the chamber is replaced by an equivalent absorbing disk of boron having a radius of 1 cm. and a mass of 1 mgm. A calculation by Skyrme (12) can then be used to estimate the perturbation, on the assumptions that the scattering medium is infinite in extent and that the neutron velocities are distributed isotropically, for a disk of mass absorption coefficient k, thickness t, and radius r. The elementary expression for the rate of neutron capture,

$$A = \pi r^2 \rho v k t,$$

is replaced by

$$A(1 - 0.03 - 0.007)$$

for the boron disk under consideration (k = 39 cm.^{2} per gm., t = 0.003 gm. per cm.^{2}, r = 1 cm.) and far from any boundary. The first term represents the 'undisturbed' rate of capture (infinitely thin detector), the second term is a function of k and t, and is consequently a property of the detector only, taking into account its finite thickness. The third term depends on the properties of the medium and of the detector, namely, it is a function of k, t, r, scattering mean free path (about 2 cm.), and the diffusion length (greater than 50 cm.) of the heavy water. Suppose that the equivalent boron disk is used in a region close to the boundary but far enough from it for the neutron velocities to be distributed almost isotropically. The rate of neutron capture in the detector will be approximately equal to $A(1 - 0.03 - f(z))$, with $f(z) \ll 0.007$ at any point z of the region investigated. In fact, the third term in the expression for the rate of absorption of neutrons is 0.007 at a distance of more than one diffusion length from the boundary and must approach zero as the boundary is approached. Consequently, this term must be less than 0.007, and it cannot change much over a distance much less than one diffusion length. The effective sensitivity of the boron chamber, which is proportional to the rate of capture of thermal neutrons, is therefore independent of z to high accuracy.*

In the Appendix some experiments using dysprosium oxide and a boron trifluoride chamber as detectors of thermal neutrons in graphite are compared. Since no significant difference in the cut-off distance was found, it is concluded that the electrical leads to the chamber do not introduce errors.

** If the equivalent boron disk is assumed to have a radius of 0.5 cm. the third term is about 0.01 inside the medium.*

Discussion of the Results

Several independent series of measurements were made; each one consisted of determining the density at various distances from the cadmium plate. In Fig. 3 the results of three typical series are plotted. One can see from the figure that the departure of $\rho(z)$ from linearity (in the region for z between

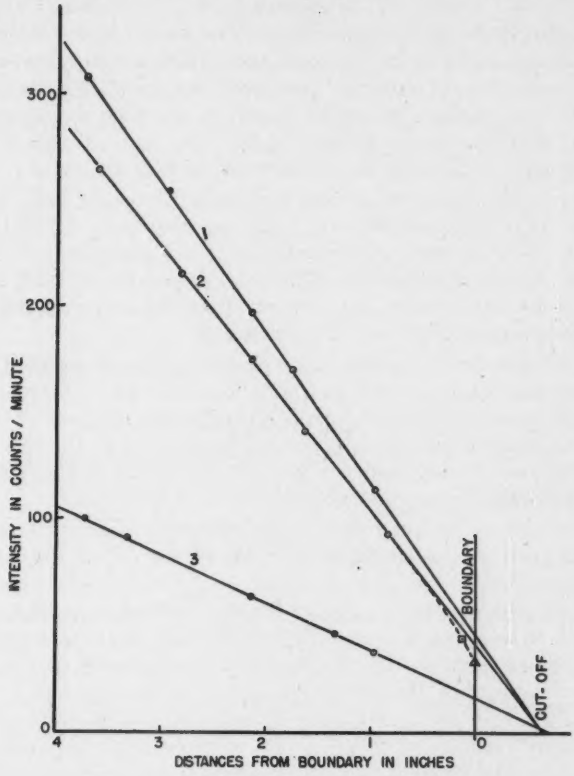

FIG. 3. *Curves representing the density of neutrons at various distances from the boundary heavy water – cadmium.*

Curve No. 1—Source 97 cm. below boundary, boron trifluoride chamber No. 1.

Curve No. 2—Source 97 cm. below boundary, boron trifluoride chamber No. 2.

Curve No. 3—Source 132 cm. below boundary, boron trifluoride chamber No. 2.

The dotted curve is the theoretical representation of the densities near the boundary. The point marked with a triangle is the theoretical value of the density at the boundary, according to Placzek and Mark. The point marked with a square is experimental.

2.5 and 9 cm.) is not detectable: this is due to the fact that the relaxation length L_r is certainly longer than 33 cm. The closest point to the boundary which was used for measuring l_t was at a distance of one mean free path from

the cadmium plate, because $\rho(z)$ is expected to depart from a straight line at distances from the boundary smaller than the transport mean free path. However, it was thought worth while to detect the curvature of $\rho(z)$ near the boundary because, to the authors' knowledge, the departure from the linearity near the boundary had never been observed. The neutron density was therefore measured when the cadmium plate was in contact with the aluminium tube ($z = 3.2$ mm.). The measured point, marked with a square in Fig. 3, is definitely below the straight line. Of course, the accuracy to which this point is measured is rather bad since here ρ is no longer a linear function of z and consequently the 'effective' position of the chamber is not accurately known. It is interesting to notice, however, that the theory predicts a departure of $\rho(z)$ from linearity about equal to the observed one (9, 10). In Fig. 3 a triangle indicates the theoretical value of ρ at the surface.

The curvature of the neutron density was roughly measured in the horizontal direction at three selected distances from the boundary. The density on the vertical axis of the tank was between 2 and 3.5% higher than at a point 9 cm. from that axis, measured along the aluminium tube. This is about the amount expected at distances over 100 cm. from the source in this graphite pile if graphite replaced the tank of heavy water.

It has been stated already that in a region where the density is linear, the effective distance between the ionization chamber and the heavy water boundary is correctly expressed by the distance from the axis of the boron trifluoride chamber to the cadmium plate, provided that the chamber has cylindrical symmetry around its geometrical axis. That this was the case is shown by the following experiments.

(1) Two series of measurements, made with two different chambers of similar construction, yielded the same value of the cut-off distance within experimental error.

(2) The effect of rotating a chamber through 180° was investigated. At a distance of 1.48 cm. from the cadmium plate, the counting rate was 85.7 ± 0.7 pulses per minute when the chamber was orientated as usual and 86.1 ± 0.7 pulses per minute when the chamber was rotated through 180°. From the slope of the straight line, at the point investigated a displacement of 1 mm. corresponds to a change in counting rate of three pulses per minute. The error in the cut-off distance is probably less than 0.3 mm. owing to this uncertainty in position, and hence is much less than the statistical error, which is given in Table I.

TABLE I

Experiment	Extrapolated cut-off distance, cm.
1	1.57 ± 0.12
2	1.63 ± 0.08
3	1.62 ± 0.08
4	1.71 ± 0.09

A straight line was fitted by the method of least squares to each of four independent sets of measurements.* The values of the cut-off distance d are given in Table I. The final results are

$$d = 1.64 \pm 0.06 \text{ cm.}$$

and

$$l_t = 2.31 \pm 0.09 \text{ cm.}$$

According to a mass spectroscopic analysis performed by Dr. H. G. Thode and his collaborators, the heavy water used in these experiments contained 99.4 atoms of deuterium per 100 atoms of hydrogen element. When a correction is applied for the neutron scattering by the light hydrogen present,† it is found that

$$l_t(100\%\ D_2O) = 2.4 \pm 0.1 \text{ cm.}$$

This value may be compared with the ordinary mean free path, which, according to several authors (2, 3, 5), is

$$l = 2 \text{ cm.}$$

It follows that

$$(\cos\theta)_{av} = 0.17,$$

with an error of about 25%.

Acknowledgments

The authors wish to thank Drs. C. Mark, G. Placzek, B. W. Sargent, and P. Wallace for their interest and co-operation.

APPENDIX

Before the measurements in heavy water were initiated, similar experiments were performed with graphite. The main purpose was to compare measurements obtained with a boron trifluoride chamber and with a dysprosium detector. The latter was a disk of aluminium, 1.6 cm. in diameter, on which was deposited 14 mgm. of dysprosium oxide. The agreement between the following results for graphite of density 1.68 gm. per cc. is seen to be satisfactory:

$d_{\text{graphite}} = 1.72 \pm 0.13$ cm. with dysprosium detector
$d_{\text{graphite}} = 1.69 \pm 0.06$ cm. with boron trifluoride chamber.

As stated at the beginning of this paper, the transport mean free path of thermal neutrons in a crystalline substance is not a well defined quantity; consequently no attempt has been made to evaluate, from the results of such experiments, the transport mean free path of thermal neutrons in graphite.

** Each density was measured to better than 1%. When the method of least squares was applied, each density was given a weight inversely proportional to the square of its absolute statistical error. The time taken to make a complete set of measurements was about 48 hr.*

† The mean free path in ordinary water is about 3.2 mm.

References

1. AMALDI, E. and FERMI, E. Phys. Rev. 50 : 899-928. 1936.
2. BEYER, H. G. and WHITAKER, M. D. Phys. Rev. 57 : 976-981. 1940.
3. CARROLL, H. Phys. Rev. 60 : 702-709. 1941.
4. FERMI, E. Ricerca sci. 7 : 13-52. 1936.
5. HANSTEIN, H. B. Phys. Rev. 59 : 489-497. 1941.
6. HEREWARD, H. G., LAURENCE, G. C., MUNN, A. M., PANETH, H. R., and SARGENT, B. W. Can. J. Research, A, 25 : 26-41. 1947.
7. HEREWARD, H. G., LAURENCE, G. C., PANETH, H. R., and SARGENT, B. W. Can. J. Research, A, 25 : 15-25. 1947.
8. MARK, C. Unpublished report, MT-26. Milne's problem for anisotropic scattering. National Research Council of Canada. 1944.
9. MARK, C. Unpublished report, MT-50. The neutron density near a plane surface. National Research Council of Canada. 1944.
10. PLACZEK, G. Unpublished report, MT-16. The neutron density near a plane surface. National Research Council of Canada. 1943.
11. PLACZEK, G. and SEIDEL, W. Unpublished report, MT-5. Milne's problem in transport theory. National Research Council of Canada. 1943.
12. SKYRME, T. H. R. Unpublished report, MS-91. Reduction in neutron density caused by an absorbing disc. British Atomic Energy Project. 1944.
13. SMYTH, H. De W. Atomic energy for military purposes. 2nd ed. Princeton Univ. Press, Princeton, N.J. 1945.
14. VEALL, N. Unpublished report, MP-60. On the construction of small boron chambers. National Research Council of Canada. 1944.

SPATIAL DISTRIBUTION OF NEUTRONS IN HYDROGENOUS MEDIA CONTAINING BISMUTH, LEAD, AND IRON[1]

By A. M. Munn[2] and B. Pontecorvo[3]

Abstract

The spatial distributions of thermal neutrons (as measured by dysprosium detectors) and of resonance neutrons (indium detectors protected by cadmium) have been investigated in several media, consisting of water and heavy elements in a heterogeneous arrangement, with two different neutron sources (Ra-α-Be and Ra-γ-Be). The experimental results are summarized in tables where the values of the mean square distances from the source of neutrons are given, for the various media, detectors, and sources used. It was found that among all the media investigated, a mixture of water and iron is the most efficient shield for neutron generating machines such as piles and cyclotrons.

Introduction

The distribution in space of slow neutrons which are produced when a source of fast neutrons is introduced in a moderating medium has been studied in a systematic way only in media containing essentially light elements, such as paraffin, water and heavy water. The object of the present work is to investigate hydrogenous substances containing high concentrations of heavy elements. The knowledge of the neutron spatial distribution in such media is not only interesting in itself, but is also very useful in solving the problem of shielding neutron generating machines such as cyclotrons and chain reacting piles. In fact, a good shield against the radiations from a neutron generating machine must combine the following properties. It must rapidly slow down neutrons and also strongly absorb the γ-radiation arising when neutrons are captured. In addition to these sources of γ-rays distributed throughout the moderating and capturing medium, in the case of the chain reacting pile the accumulated fission products emit strong γ-radiation. The necessity for strong absorption of γ-radiation by the shield suggests heavy elements. The choice is further limited by the requirement that the material must be inexpensive, for in a practical case the quantity needed may be very large. On these grounds iron and lead should be considered. On the other hand, the need for an efficient and inexpensive moderator for neutrons suggests immediately a substance containing hydrogen, such as water or wood. A mixture of water with iron or lead should therefore be a good shield against both neutrons and γ-rays. Mixtures of water with bismuth are also interesting for the general understanding of the process of moderation and diffusion of neutrons.

[1] *Manuscript received October 16, 1946.*

Contribution from the Montreal Laboratory, Nuclear Physics Branch, Division of Atomic Energy, National Research Council of Canada. (Work performed in 1943.) Issued as N.R.C. No. 1525.

[2] *Physicist; now at McGill University, Montreal, Que.*

[3] *Member of the United Kingdom staff, now at the Chalk River Laboratory, Chalk River, Ont.*

In a discussion of the effect of heavy atoms in a hydrogenous material on the spatial distribution of neutrons, two points should be kept in mind. First, if fast neutrons are scattered inelastically by the heavy nuclei, the slowing down efficiency is increased. The spatial distribution of slow neutrons around a source in the scattering medium may therefore be affected by inelastic collisions if the neutrons from the source are sufficiently energetic. The neutrons from a mixed radium and beryllium source (Ra-α-Be) are certainly sufficiently energetic and undergo inelastic collisions against heavy nuclei. On the contrary, the photoneutrons from a radium and beryllium source (Ra-γ-Be), having a much smaller energy, may be incapable of exciting nuclei and undergoing inelastic collisions. Secondly, elastic collisions must be considered. Although a neutron loses a small fraction of its energy in an elastic collision with a heavy nucleus, the effect of such collisions upon their spatial distribution is far from negligible for the following reasons. (1) Since the elastic scattering cross-section of a heavy element does not decrease with increasing energy of the neutrons as rapidly as in the case of hydrogen, collisions against the heavy nuclei are comparatively frequent at high energies. (2) After neutrons make collisions against heavy nuclei, their velocities are distributed isotropically, while in the case of hydrogen their velocities are predominantly forward.

The effect of elastic collisions in nuclei heavier than hydrogen was first described by Fermi (4) in his original theoretical derivation of the mean square distance of neutrons in water. The effects of inelastic and elastic scattering collisions of neutrons with heavy nuclei will be discussed in detail later.

In the absence of inelastic collisions, in principle, the mean square distance of neutrons of a given energy from a source of fast neutrons embedded in a scattering medium could be calculated. Prerequisite data, such as the energy distribution of the neutrons from the source and the scattering cross-sections of all types of nuclei present at various energies of the neutrons, are however not well known. Under these circumstances, a simple experimental approach seemed likely to yield information of theoretical and practical value in a short time. Since high concentrations of the elements iron, lead, and bismuth in water were required, solutions of their compounds could not be used. A heterogeneous mixture, and a lattice, resembling a checkerboard, of water and the heavy element was adopted. The spatial distributions of thermal and indium resonance neutrons were explored in several lattices using two different sources of fast neutrons (Ra-α-Be) and (Ra-γ-Be).

Experimental Method

The Ra-α-Be source consisted of 1 gm. of radium bromide mixed with beryllium, enclosed by a brass cylinder of radius 1.8 cm. and height 1.8 cm. The Ra-γ-Be source consisted of 1 gm. of radium at the middle of a cube of beryllium, 4.9 cm. edge. This cube had to be large in order to get sufficient neutron intensity, although its size makes the results more difficult to interpret.

The experimental arrangement is shown in Fig. 1. The tank was made of galvanized iron, painted on the inside to prevent corrosion. Its dimensions were: 90 cm. long, 45 cm. wide, and 45 cm. deep. The square rods, arranged in a checkerboard pattern, were supported on end in the tank by a grid of wires. The lead and bismuth rods were 32 by 2 by 2 cm. and the iron rods 32 by 1.87 by 1.87 cm. The latter were nickel plated. The depth of water in the tank was 32 cm. By varying the arrangement of the rods, various ratios of volume of water to metal could be obtained (1 : 2, 1 : 1, 2 : 1 for bismuth and lead, 1.3 : 1 for iron).

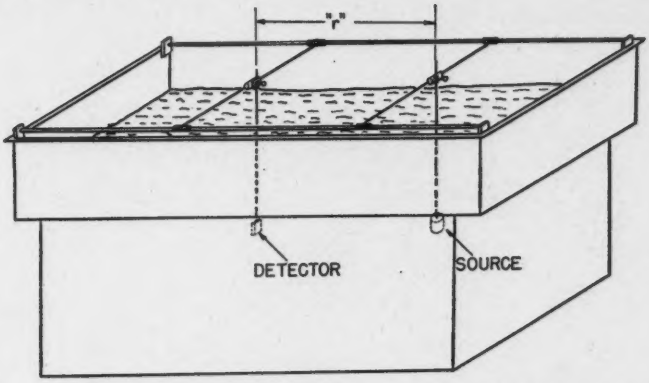

FIG. 1. *Sketch of the tank, in which $H_2O + Bi$, $H_2O + Pb$, $H_2O + Fe$ lattices were studied in a checkerboard arrangement.*

The source and the boxes for the detectors were supported by a system giving three dimensional motion. These were placed halfway down in the water. The source was placed in a fixed position about 20 cm. from one end of the tank, while the detectors were irradiated at various distances r from the centre of the source, measured in several directions. The minimum distance between a detector and the nearest boundary of the mixture of water and metal was 15 cm.

The detectors of thermal neutrons consisted of 70 mgm. each of dysprosium oxide on an aluminium tray, 2 by 2.5 cm. The detectors of resonance neutrons were made of indium, 45 mgm. each on an aluminium backing, 2 by 2.5 cm. The dysprosium detectors were activated in flat watertight aluminium boxes, the indium in similar cadmium boxes of wall thickness 0.6 mm. Following the irradiation of the detectors by neutrons, their β-activities were measured on a thin-walled aluminium counter. Corrections were applied for decay during measurement and lack of saturation at the end of the irradiation, using 138 and 54 min. respectively for the half-periods of dysprosium and indium.

Experimental Results

Let I represent the saturation β-activity of a detector, measured in counts per minute of the Geiger–Müller counter, after the detector has been exposed to neutrons at a distance r from the source. Now, I is directly proportional to the density of thermal neutrons in the case of a dysprosium detector or to the density of resonance neutrons in the case of an indium detector under cadmium. The number of neutrons of the type considered found in a shell of constant thickness and mean radius r about the source is therefore directly proportional to Ir^2, if the system is spherically symmetrical. A plot of Ir^2 against r is a convenient way of representing the spatial distribution (1). Examples are shown in Figs. 2 and 3.

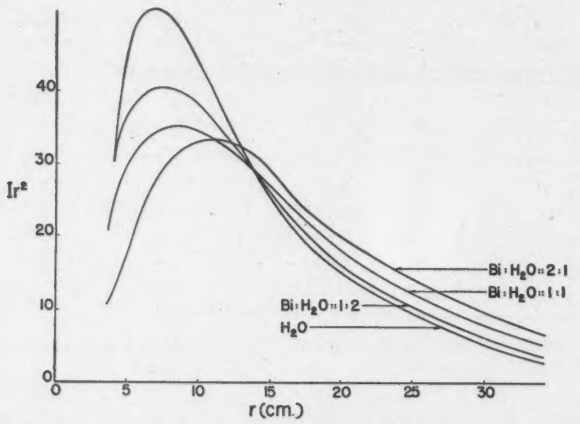

FIG. 2. *Spatial distribution of In resonance neutrons. Source: Ra-α-Be.*

Although some detail is sacrificed in the process, a single parameter is usually derived from the spatial distribution, for convenience in discussion. This parameter is the mean square distance from the source, $(r^2)_{av}$, of the neutrons of the type considered. A characteristic length L_c in the medium, simply related to $(r^2)_{av}$, may be defined for convenience. The mean square distance is found from the obvious relation:

$$(r^2)_{av} = 4\pi \int_0^\infty I(r) r^4 dr \Big/ 4\pi \int_0^\infty I(r) r^2 dr \, . \tag{1}$$

The characteristic length L_c is defined by

$$L_c^2 = \frac{1}{6} (r^2)_{av} \, . \tag{2}$$

The following assumptions are implied: (1) the source is effectively a point, (2) the material of the source has the same slowing down properties as the

mixture of water and metal, and (3) the neutron density is spherically symmetrical around the source, as it would be if the medium were homogeneous. The last assumption holds sufficiently well, for the tank was large enough and the neutron densities were measured at corresponding points in the lattice.

The experimental results are summarized in Tables I and II. The Ra-α-Be source conforms sufficiently to the assumption of a point source, but the Ra-γ-Be source does not. The geometrical error in the mean square distance caused by the departure of the source distribution from a point is estimated at less than 10% for the beryllium cube in any of the media investigated. The correction for the difference in the slowing down properties of beryllium and

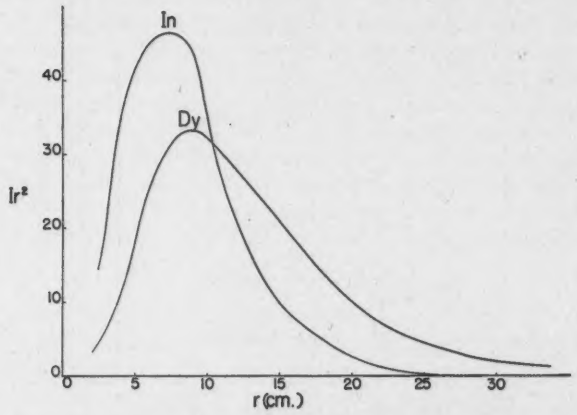

FIG. 3. *Spatial distribution of resonance neutrons (In) and of thermal neutrons (Dy) in H_2O + Bi (1 : 1 by volume). Source: Ra-γ-Be. (The side of the Be cube is 4.9 cm.)*

the surrounding medium was more serious and was estimated as follows. The average energy of the photoneutrons was assumed to be 130 kev. According to a calculation by Marshak (7), which was based on known scattering cross-sections, $(r^2)_{av}$ = 38 cm.^{2} in water for neutrons of energy 130 kev. This value is 20 cm.^{2} smaller than the measured 58 cm.^{2} in water (Table II). The slowing down properties of the mixtures of water and metal are more similar to those of water than to those of beryllium. A rough order of magnitude calculation indicates that the correction is about 18 cm.^{2} for all the media investigated. The observed values of $(r^2)_{av}$ in Table II have been reduced by 18 cm.^{2}

Since the measurements could not be carried out at very large values of r, owing to lack of intensity, some extrapolation of the spatial distribution was necessary in evaluating $(r^2)_{av}$. At large values of r the quantity Ir^2 decreases according to $e^{-r/\lambda}$, where λ, defined as the relaxation length, is an important parameter in shielding considerations. Although in fact λ increases slowly

with r, for the purpose of extrapolation λ was estimated at the last part of the measured distribution, and Ir^2 assumed to decrease with this relaxation length.

TABLE I

SOURCE: RA-α-BE

Medium (volume ratio)	Concentrations, C, gm-atoms/l.	Detector	$(r^2)_{av}$, cm.^{2}	L_c, cm.
H_2O	$C_H = 111$	Dy	330	7.4 ± 0.2
*H_2O	$C_H = 111$	Rh(Cd difference)	327	7.4
H_2O	$C_H = 111$	In resonance	278	6.8 ± 0.2
*H_2O	$C_H = 111$	Rh resonance	277	6.8
H_2O : Bi :: 1 : 1	$C_H = 56$ $C_{Bi} = 23$	Dy	562	9.7 ± 0.4
H_2O : Bi :: 2 : 1	$C_H = 74$ $C_{Bi} = 15$	In resonance	398	8.1 ± 0.3
H_2O : Bi :: 1 : 1	$C_H = 56$ $C_{Bi} = 23$	In resonance	477	8.9 ± 0.4
H_2O : Bi :: 1 : 2	$C_H = 37$ $C_{Bi} = 30$	In resonance	517	9.3 ± 0.4
H_2O : Pb :: 1 : 1	$C_H = 56$ $C_{Pb} = 27$	In resonance	437	8.5 ± 0.3
H_2O : Fe :: 1.3 : 1	$C_H = 63$ $C_{Fe} = 60$	In resonance	319	7.3 ± 0.3

* *Measured by Amaldi and Fermi (1), using a Rn-α-Be source.*

TABLE II

SOURCE: RA-γ-BE

DETECTOR: IN UNDER CD

Medium (volume ratio)	Concentrations, C, gm-atoms/l.	$(r^2)_{av}$, cm.^{2}		L_c, cm.
		Observed	Corrected	
H_2O	$C_H = 111$	58	38	2.5
H_2O : Bi :: 2 : 1	$C_H = 74$ $C_{Bi} = 15$	87	69	3.4
H_2O : Bi :: 1 : 1	$C_H = 56$ $C_{Bi} = 23$	95	77	3.6
H_2O : Pb :: 1 : 1	$C_H = 56$ $C_{Pb} = 27$	87	69	3.4
H_2O : Fe :: 1.3 : 1	$C_H = 63$ $C_{Fe} = 60$	79	61	3.2

In conclusion, it should be emphasized that the values of $(r^2)_{av}$ in Tables I and II are by no means equally accurate. Since the Ra-α-Be source has small dimensions and the values of $(r^2)_{av}$ are comparatively high, Table I is satisfactory. On the other hand, Table II is unsatisfactory for the opposite reasons, and only close comparisons of $(r^2)_{av}$ within the table should be attempted. No attempt was made to estimate the error affecting the values of L_c in Table II.

Discussion

The values of $(r^2)_{av}$ and L_c for *C* or cadmium absorbable neutrons and for rhodium resonance neutrons obtained with a Rn-α-Be source in water by Amaldi and Fermi (1) are included in Table I. The agreement with the present results is very good.

It is seen that the characteristic length L_c is greater when dysprosium is used as a detector of neutrons than when indium shielded by cadmium is used, the source and medium being the same (Table I). This is due to the fact that the motion of neutrons consists of two phases: (i) the slowing down phase, where the neutrons are slowed down from their average initial energy to the beginning of the thermal energy region, which is associated with a characteristic length L_s called the slowing down length, and (ii) the diffusion phase, associated with a characteristic length L called the diffusion length. Since dysprosium detects thermal neutrons, it is easy to see that with this detector

$$L_c^2(\text{Dy}) = L_s^2 + L^2.$$

In the case of the indium detector shielded by cadmium, the neutrons are detected at the resonance energies of indium that lie above the strong absorption region of cadmium. The strongest resonance band of indium is at 1.44 ev. The characteristic length L_c is therefore the slowing down length to 1.44 ev., which may be called $L_s'(<L_s)$. Since the squares of such lengths are additive,

$$L_c^2(\text{Dy}) - L_c^2(\text{In}) = L_s^2 + L^2 - L_s'^2,$$

which qualitatively explains the differences noted above for water and a mixture of water and bismuth. The difference for water and bismuth is much greater than the difference for water (first observed and explained by Amaldi and Fermi (1)), because of the increase in the diffusion length when bismuth replaces part of the water, the capture cross-section of bismuth for thermal neutrons being low.

The very great difference in the spatial distributions of thermal and indium resonance neutrons may be seen directly. The greater spread of the former is shown in Fig. 3, where the two are compared in a lattice of water and bismuth around a Ra-γ-Be source. (Owing to the perturbation by the mass of beryllium, the mean square distance of thermal neutrons has been omitted from Table II.)

For a further discussion of the experimental results in Tables I and II it will be convenient to use values of the scattering cross-sections in hydrogen, iron, lead, and bismuth for neutrons of several energies (2, 3, 5, 6). From

these, given in Table III, the scattering mean free paths of Table IV were calculated for the mixtures of water and metal used in these experiments. Although the lattice spacings are comparable to the scattering mean free paths, it is necessary to ignore the heterogeneity and consider each lattice replaced by a homogeneous medium having the same atomic composition and density.

TABLE III

SCATTERING CROSS-SECTIONS σ (IN UNITS OF 10^{-24} CM.^{2}) AT VARIOUS NEUTRON ENERGIES FOR THE SUBSTANCES DENOTED BY THEIR CHEMICAL SYMBOLS

Neutron energy, ev.	σ				
	H	H_2O	Fe	Pb	Bi
1	20.5	46.0	11.1	9.6	8.7
130×10^3	11.5	28.6	3.5	7.3	8.1
220×10^3	8.0	24.0	3.6	6.2	8.4
460×10^3	6.3	16.6	—	5.8	6.7
900×10^3	4.5	13.8	3.1	5.1	5.4
2.7×10^6	2.5	6.0	3.1	6.4	6.5
3×10^6	2.3	5.6	—	6.7	6.7
5×10^6	1.6	4.6	—	—	—

TABLE IV

SCATTERING MEAN FREE PATH, IN CM., IN HOMOGENEOUS MEDIA HAVING THE SAME ATOMIC COMPOSITION AND DENSITY AS THE LATTICES INVESTIGATED

Neutron energy, ev.	Scattering mean free path, cm.					
	H_2O	H_2O + Bi (2 : 1)	H_2O + Bi (1 : 1)	H_2O + Bi (1 : 2)	H_2O + Fe (1.3 : 1)	H_2O + Pb (1 : 1)
1	0.65	0.98	1.1	1.4	0.8	1.05
130×10^3	1.05	1.4	1.7	2.1	1.5	1.7
220×10^3	1.25	1.6	1.9	2.3	1.7	2.0
460×10^3	1.80	2.3	2.6	3.2	—	2.7
900×10^3	2.15	2.7	3.2	3.8	2.7	3.2
3×10^6	5.3	5.3	5.4	5.4	4.7	4.9
5×10^6	6.5	—	—	—	—	—

It is worth while mentioning the following points.

(1) The spatial distributions in Fig. 2 and Tables I and II show that the mean square distance is increased when iron, lead, or bismuth is added to water. This observation is in qualitative agreement with the increase in the mean free path which is caused by the addition of the metal (Table IV) for all but the very high neutron energies.

(2) The least values of $(r^2)_{av}$ obtained in the hydrogenous media containing heavy metals were those for water and iron (Tables I and II), which fact is to be explained by the high atomic concentration in iron and the consequently reduced mean free path (Table IV).

(3) The ratio R of the mean square distance obtained with a Ra-α-Be source to that obtained with a Ra-γ-Be source is smallest in water and iron (Table V). This fact indicates that probably inelastic collisions are relatively most important in iron. However, no certain conclusion can be drawn on this point, since the smallness of the mean free path at very high neutron energy

TABLE V

DETECTOR: IN UNDER CD

$$R = \frac{(r^2)_{av}(\text{Ra-}\alpha\text{-Be})}{(r^2)_{av}(\text{Ra-}\gamma\text{-Be})}$$

Medium	R
H_2O	7.3
H_2O : Bi ::2 : 1	5.8
H_2O : Bi ::1 : 1	6.2
H_2O : Pb ::1 : 1	6.3
H_2O : Fe ::1.3 : 1	5.2

in water and iron might be sufficient to explain the observations. The fact that the highest value of R is in water is due to the very rapid increase of the mean free path with the neutron energy, characteristic of hydrogen.*

(4) The shielding properties of a medium for neutrons are determined jointly by the mean square distance and the relaxation length at large distances. In the lattices of water and bismuth and water and lead the relaxation lengths at large distances from the Ra-α-Be source are larger than that in water. On the other hand, in the lattice of water and iron the relaxation length (9.4 cm.) is somewhat smaller than—more exactly within experimental error equal to—the value in water. At greater distances from the source than those that could be used in the experiment, the 'hardening' of the radiation should be more pronounced in water than in water and iron for the following reasons. The cross-section of very energetic neutrons is low in hydrogen but fairly high in iron, and inelastic collisions in iron become important for energetic neutrons. It is clear, therefore, that water and iron constitutes a very good shield for neutron generating machines.

It is possible to estimate the mean square distance of neutrons of a given energy on the basis of Fermi's age-velocity theory. Unfortunately, in the case of hydrogenous media, the scattering mean free path of energetic neutrons changes too rapidly for a change of the neutron energy corresponding to the average energy loss per collision. For this reason the age-velocity theory will be more reliable for the photoneutrons from a Ra-γ-Be source than for the more energetic neutrons from a Ra-α-Be source.

** Incidentally it seems worth while to point out here that water would be completely inadequate for shielding very high energy neutrons produced by the newly developed frequency modulated cyclotrons. Water and iron, on the contrary, appears to be very promising for shielding such instruments.*

Suppose the source is emitting neutrons of average initial energy E_i in a medium composed of elements of several types k. The following symbols are needed:

M_k = nuclear mass of type k,

C_k = atomic concentration for type k,

a_k = average logarithmic energy loss in elastic collisions (8) between neutrons and nuclei of type k ($a_{\text{hydrogen}} = 1$, $a_{\text{oxygen}} = 0.12$, $a_{\text{iron}} = 0.036 \ldots$),

$\sigma_k(E')$ = total cross-section of nuclei of type k at the neutron energy E',

$l(E')$ = total mean free path in the medium for neutrons of energy E',

$p_k(E')$ = probability that a neutron of energy E' makes a collision with a nucleus of type k,

$$p_k(E') = \frac{C_k\sigma_k(E')}{\Sigma C_k\sigma_k(E')} .$$

The mean square distance traversed by neutrons in slowing down from E_i to E, on the age-velocity theory, is given by

$$(r^2)_{av} = 2\int_E^{E_i} \frac{l^2(E')\,dE'}{(\Sigma p_k a_k)\left(1 - \frac{2}{3}\Sigma\frac{p_k}{M_k}\right)E'} . \tag{3}$$

Owing to the small loss of energy in collisions with heavy nuclei and their large mass in comparison with hydrogen, Equation (3) can be written in the simple approximate form:

$$(r^2)_{av} = 2\int_E^{E_i} \frac{l^2(E')\,dE'}{p_H(1 - \frac{2}{3}\,p_H)\,E'} . \tag{4}$$

Using the values of the cross-sections given in Table III, p_H and $p_H(1 - \frac{2}{3}\,p_H)$ as shown in Table VI were obtained. The quantity p_H can vary only between zero (no hydrogen) and unity (pure hydrogen), and the quantity $1 - \frac{2}{3}\,p_H$ between unity and 0.33. Consequently, the quantity $p_H(1 - \frac{2}{3}\,p_H)$ rises from zero where $p_H = 0$ and eventually reaches a flat maximum of 0.37 at $p_H = 0.75$. As shown in Table VI, $p_H(1 - \frac{2}{3}\,p_H)$ is practically constant at 0.37 in all media used in the experiments, for neutron energies from 1 volt to 100 kev. Consequently, for neutrons from a Ra-γ-Be source, this part of the denominator of the integral (Equation (4)) can be taken outside the integral sign, *leaving $(r^2)_{av}$ dependent on the medium only through the mean free path.*

If the ratio

$$\frac{(r^2)_{av}(\text{H}_2\text{O} + \text{heavy element})}{(r^2)_{av}(\text{H}_2\text{O})}$$

of the experimental, corrected values of the mean square distances given in Table II is compared with the ratio of the square of the 'average' mean free path at low energies in the corresponding media (Table IV), qualitative agreement is found, within the various experimental errors and approximations involved.

TABLE VI

VALUES OF p_H AND $p_H(1 - \frac{2}{3} p_H) = q_H$ FOR HOMOGENEOUS MEDIA HAVING THE SAME ATOMIC COMPOSITION AS THE HETEROGENEOUS ONES INVESTIGATED

Neutron energy, ev.	H_2O		H_2O + Bi (2 : 1)		H_2O + Bi (1 : 1)		H_2O + Bi (1 : 2)		H_2O + Fe (1.3 : 1)		H_2O + Pb (1 : 1)	
	p_H	q_H	p_H	q_H	p_H	q_H	p_H	q_H	p_H	q_H	p_H	q_H
1	0.89	0.36	0.83	0.37	0.77	0.37	0.68	0.37	0.60	0.36	0.74	0.37
130×10^3	0.81	0.37	0.72	0.37	0.66	0.37	0.55	0.35	0.64	0.37	0.64	0.37
220×10^3	0.67	0.37	0.59	0.36	0.52	0.34	0.43	0.31	0.52	0.34	0.53	0.35
460×10^3	0.76	0.37	0.65	0.37	0.57	0.36	0.46	0.32	—	—	0.57	0.36
900×10^3	0.65	0.37	0.56	0.35	0.50	0.33	0.40	0.29	0.45	0.32	0.47	0.32
2.7×10^6	0.83	0.37	0.58	0.36	0.44	0.31	0.31	0.25	—	—	0.41	0.29
3×10^6	0.83	0.37	0.56	0.35	0.42	0.30	0.29	0.23	0.39	0.29	0.38	0.28
5×10^6	0.70	0.37	—	—	—	—	—	—	—	—	—	—

Acknowledgments

The authors wish to thank Dr. H. Halban and Dr. B. W. Sargent for their interest and co-operation.

References

1. AMALDI, E. and FERMI, E. Phys. Rev. 50 : 899-928. 1936.
2. BRETSCHER, E. and MURRELL, E. B. M. Unpublished report, Br-136. The total neutron collision areas of some heavy metals. British Atomic Energy Project. 1943.
3. BRETSCHER, E. AND MURRELL, E. B. M. Unpublished report, Br-137. Determination of the total neutron collision cross-section for hydrogen and carbon. British Atomic Energy Project. 1943.
4. FERMI, E. Ricerca sci. 7 : 13-52. 1936.
5. HANSTEIN, H. B. Phys. Rev. 59 : 489-497. 1941.
6. LEIPUNSKY, A. I. J. Phys. U.S.S.R. 3 : 230-236. 1940.
7. MARSHAK, R. E. Unpublished report, MT-17. On the slowing-down length of neutrons in water. National Research Council of Canada. 1944.
8. PLACZEK, G. Phys. Rev. 69 : 423-438. 1946.

CANADIAN JOURNAL OF RESEARCH

Notes on the Preparation of Copy

GENERAL:—Manuscripts should be typewritten, double spaced, and the **original and at least one extra copy** submitted. Style, arrangement, spelling, and abbreviations should conform to the usage of this Journal. Names of all simple compounds, rather than their formulae, should be used in the text. Greek letters or unusual signs should be written plainly or explained by marginal notes. Superscripts and subscripts must be legible and carefully placed. Manuscripts should be carefully checked before being submitted, to reduce the need for changes after the type has been set. **All pages, whether text, figures, or tables, should be numbered.**

ABSTRACT:—**An abstract of not more than about 200 words, indicating the scope of the work and the principal findings, is required.**

ILLUSTRATIONS:

(i) *Line Drawings:*—All lines should be of sufficient thickness to reproduce well. Drawings should be carefully made with India ink on white drawing paper, blue tracing linen, or co-ordinate paper **ruled in blue only**; any co-ordinate lines that are to appear in the reproduction should be ruled in black ink. Paper ruled in **green, yellow, or red should not be used** unless it is desired to have all the co-ordinate lines show. Lettering and numerals should be neatly done in India ink preferably with a stencil (**do not use typewriting**) and be of such size that they will be legible and not less than one millimetre in height when reproduced in a cut three inches wide. All experimental points should be carefully drawn with instruments. Illustrations need not be more than two or three times the size of the desired reproduction, but the ratio of height to width should conform with that of the type page. **The original drawings and one set of small but clear photographic copies are to be submitted.**

(ii) *Photographs:*—Prints should be made on glossy paper, with strong contrasts; they should be trimmed to remove all extraneous material so that essential features only are shown. Photographs should be submitted **in duplicate**; if they are to be reproduced in groups, one set should be so arranged and mounted on cardboard with rubber cement; the duplicate set should be unmounted.

(iii) *General:*—**The author's name, title of paper, and figure number should be written on the back of each illustration.** Captions should not be written on the illustrations, but typed on a separate page of the manuscript. All figures (including each figure of the plates) should be numbered consecutively from 1 up (arabic numerals). **Each figure should be referred to in the text.**

TABLES:—Titles should be given for all tables, which should be numbered in Roman numerals. Column heads should be brief and textual matter in tables confined to a minimum. **Each table should be referred to in the text.**

REFERENCES:—**These should be listed alphabetically by authors' names, numbered in that order, and placed at the end of the paper.** The form of literature citation should be that used in this Journal. **Titles of papers should not be given in references listed in Sections A, B, E, and F, but must be given in references listed in Sections C and D. All citations should be checked with the original articles.** Each citation should be referred to in the text by means of the key number; in Sections C and D the author's name and the date of publication may be included with the key number if desired.

The *Canadian Journal of Research* conforms in general with the practice outlined in the *Canadian Government Editorial Style Manual*, published by the Department of Public Printing and Stationery, Ottawa.

Reprints

Fifty reprints of each paper are supplied free. Additional reprints, if required, will be supplied according to a prescribed schedule of charges.